Geophys. J. Int. (2009) **178,** 23–46 doi: 10.1111/j.1365-246X.2009.04185.x

GJI Geodesy, potential field and applied geophysics

Crustal motions in Great Britain: evidence from continuous GPS, absolute gravity and Holocene sea level data

F. N. Teferle,[1] R. M. Bingley,[1] E. J. Orliac,[1] S. D. P. Williams,[2] P. L. Woodworth,[2] D. McLaughlin,[2] T. F. Baker,[2] I. Shennan,[3] G. A. Milne,[4,*] S. L. Bradley[4] and D. N. Hansen[1]

[1]*Institute of Engineering Surveying and Space Geodesy, University of Nottingham, Nottingham, UK. E-mail: norman.teferle@nottingham.ac.uk*
[2]*Proudman Oceanographic Laboratory, Liverpool, UK*
[3]*Department of Geography, Durham University, Durham, UK*
[4]*Department of Earth Sciences, Durham University, Durham, UK*

Accepted 2009 March 19. Received 2009 March 18; in original form 2008 July 16

SUMMARY

Two independent continuous global positioning system (CGPS) processing strategies, based on a double-difference regional network and a globally transformed precise point positioning solution, provide horizontal and vertical crustal motion estimates for Great Britain. Absolute gravity and geological information from late Holocene sea level data further constrain the vertical motion estimates. For 40 CGPS stations we estimate station velocities and associated uncertainties using maximum likelihood estimation, assuming the presence of white and coloured noise. Horizontal station velocity estimates agree to <1 mm yr^{-1} between the two CGPS processing strategies and closely follow predicted plate motions. Residual velocities, generally <1 mm yr^{-1}, follow no regular pattern, that is, there is no discernible internal deformation, nor any dependence on station monumentation or time-series length. Vertical station velocity estimates for the two CGPS processing strategies agree to ∼1 mm yr^{-1}, but show an offset of ∼1 mm yr^{-1} with respect to the absolute gravity (AG) estimates. We attribute this offset to a bias related to known issues in current CGPS results and correct for it by AG-alignment of our CGPS estimates of vertical station velocity. Both CGPS estimates and AG-aligned CGPS estimates of present-day vertical crustal motions confirm the pattern of subsidence and uplift in Great Britain derived from Holocene sea level data for the last few thousand years: ongoing subsidence on Shetland, uplift in most areas of Scotland, and subsidence in large areas of England and Wales.

Key words: Time series analysis; Satellite geodesy; Time variable gravity; Plate motions; Europe.

1 INTRODUCTION

1.1 Context

There are two large-scale geophysical processes known to cause crustal motions in Great Britain. The first, the motion of the Eurasian plate due to plate tectonics, predominantly acts on the horizontal coordinate components with negligible effect on the vertical. The second, known as glacial isostatic adjustment (GIA), is the on-going viscous response of the solid Earth to past changes in ice sheets and sea level. This process contributes a signal in both the vertical and horizontal components (e.g. Mitrovica *et al.* 1994; Milne *et al.* 2001, 2006).

The plate tectonics signal in Great Britain, a rotation along with the Eurasian plate, is seen as motion in a northeasterly direction of approximately 23 mm yr^{-1}. Great Britain is considered part of the rigid interior of the Eurasian plate, although some residual motion of southeast England with respect to central Europe has been reported previously (Nocquet *et al.* 2001; Nocquet & Calais 2003). Apart from this, there have been few studies concerned with the plate motion signal or the stability of the plate within Great Britain due to a lack of geodetic data.

In contrast to plate motions, the GIA signal has been studied in great detail in the area of Great Britain. The majority of studies to date have considered only the sea level aspect of the GIA signal (e.g. Lambeck 1993a,b; Lambeck *et al.* 1996; Peltier *et al.* 2002; Shennan *et al.* 2002). As the precision of geodetic constraints from continuous global positioning system (CGPS) measurements have improved, these data have been employed more recently in GIA modelling studies (e.g. Milne *et al.* 2006). With regard to the

*Now at: Department of Earth Sciences, University of Ottawa, Canada.

crustal motion signal recorded by CGPS, the data provide a good test of the models through the summation of both the near and far-field effects. In general, the signal manifests itself as a combination of the effects related to the deglaciation of the Laurentide, Fennoscandian and the British–Irish ice sheets (Milne *et al.* 2006). For the horizontal components, the dominant signal is associated with the Laurentide ice sheet and is predicted to be in a northwesterly direction. The magnitude of the horizontal GIA signal varies across the region and is thought to be of the order of 1–2 mm yr^{-1} (Milne *et al.* 2006). For the vertical component, the dominant signal is associated with the British–Irish ice sheet and the adjacent, significantly larger Fennoscandian ice sheet, resulting in subsidence on Shetland, uplift in most areas of Scotland, and subsidence in large areas of England and Wales. Prior to the availability of CGPS measurements, vertical crustal motion was inferred from geological information of relative sea level change, inverted to form maps of Holocene crustal movements (Shennan 1989; Shennan & Horton 2002; Shennan *et al.* 2006). As changes in sea level around Great Britain are of major concern, it is this geological information which has so far been used to correct tide gauge (TG) records for changes in land levels (e.g. Woodworth *et al.* 1999).

On a local scale, past crustal motions occurred along the main fault systems in Scotland (e.g. Curry 1986; Canning *et al.* 1998; Stewart *et al.* 2001), but these motions are believed to have largely ceased. Whereas, more recent neotectonic crustal motions have been reported for London in southeast England (Ellison *et al.* 2004). Similarly, in some areas we may also expect to see subsidence associated with sediment compaction (e.g. Zong & Tooley 1996; Shennan & Horton 2002; Edwards 2006; Hill *et al.* 2007) and the extended deep mining activities throughout the Anthropocene (e.g. Humphries 2001; Bell *et al.* 2005; Donnelly 2006). Although it is worth noting that most deep mining ended in the 1980s and the current geodetic monitoring network of CGPS and absolute gravity (AG) stations were established in the late 1990s.

For many years the only CGPS station in Great Britain was located at Herstmonceux in southeast England. In the late 1990s other CGPS stations were established, predominantly at sites of the national TG network. The main objective of these was to measure the vertical land motions directly at the TG sites (Teferle *et al.* 2002, 2006; Teferle 2003). We note here that such CGPS@TG stations may not only be affected by large-scale vertical crustal motions and local scale subsidence, but also by local instabilities, as these stations are often founded on structures such as piers and quays of varying age and foundations.

Initially the CGPS network grew slowly, as expansion was mainly driven by various scientific objectives, similar to those in Scandinavia (e.g. Milne *et al.* 2001; Johansson *et al.* 2002; Lidberg *et al.* 2007) . However, since the year 2000, a larger number of CGPS stations were established as network real-time kinematic (RTK) CGPS stations, but mainly located on buildings.

To advance sea level research, in the late 1990s three AG stations were also established near TGs (Williams *et al.* 2001). In contrast to the CGPS@TG stations, these were located in buildings believed to be founded on bedrock, thus providing estimates of vertical crustal motions. That AG is an essential technique when investigating such motions has been shown previously (e.g. Larson & van Dam 2000; Lambert *et al.* 2001; Mazzotti *et al.* 2007). In terms of accuracy, the role of AG is also becoming critical for the vertical component, as a geodetic technique independent of the International Terrestrial Reference Frame (ITRF), namely ITRF2000 (Altamimi *et al.* 2002) and its update ITRF2005 (Altamimi *et al.* 2007).

Although much work has been undertaken to improve the precision of vertical crustal motions from CGPS, the absolute accuracy of these is currently still limited by the accuracy of the ITRF, which is ∼2 mm yr^{-1} in the vertical. This limitation stems from difficulties in the accurate determination of the geocentre of the ITRF and its long-term motion with respect to the centre of mass (CM) of the Earth system (e.g. Wu *et al.* 2002; Blewitt 2003; Dong *et al.* 2003; Argus 2007).

In recent discussions, the accuracy of horizontal crustal motions from CGPS has also been questioned. These may only be accurate at the 1–2 mm yr^{-1} level due to the implementation of the no-net rotation condition in ITRF2000 and ITRF2005 (Kreemer *et al.* 2006; Altamimi *et al.* 2007). Additionally, estimates from regional realizations of the terrestrial reference frame, still implemented in many studies, may be biased/offset, depending on the subset of reference frame sites used for the regional reference frame implementation (Dong *et al.* 2003; Mazzotti *et al.* 2008).

In response to these issues, Aoki & Scholz (2003) computed absolute vertical station velocities by alignment of their CGPS estimates to those estimated at 18 TGs in the Japanese Islands, assuming a global averaged sea level rise of 1.8 mm yr^{-1}. Caccamise *et al.* (2005) reported only relative and not absolute vertical station velocity estimates between several CGPS stations in Hawaii, and Bennett & Hreinsdóttir (2007) determined a local vertical reference frame using Holocene and Late Pleistocene geological evidence of vertical crustal motions. A similar, but alternative approach has been advocated for the CGPS@TG stations in Great Britain based on an alignment of the CGPS vertical station velocity estimates to those from AG (Teferle 2003; Teferle *et al.* 2006). The advantage of this approach lies in the nature of these two complementary geodetic techniques giving independent estimates over a comparable time span if operated in parallel.

In addition to problems with the terrestrial reference frame, it is well known that CGPS coordinate solutions suffer from residual errors due to inaccurate models of systematic biases both directly, when these are applied by the user, and indirectly through the use of GPS satellite orbit and clock, and Earth rotation products. For example, significant effects on the vertical coordinate component have been reported due to inadequate modelling of satellite and receiver antenna phase centres (e.g. Ge *et al.* 2005; Cardellach *et al.* 2007), the neglecting of higher-order ionospheric terms (Kedar *et al.* 2003; Fritsche *et al.* 2005; Hernández-Pajares *et al.* 2007), the inadequate modelling of the tropospheric delay (e.g. Böhm *et al.* 2006; Vey *et al.* 2006), and the effect of different loading processes (e.g. van Dam *et al.* 2001; Tregoning & Van Dam 2005). The benefits of improved models from some of this recent research have been demonstrated in a re-analysis of global CGPS data set for the period between 1994 and 2005 (Steigenberger *et al.* 2006). However, such improved models are not always readily available to users of different GPS software, or accounted for in the current GPS satellite orbit and clock, and Earth rotation products available from the International GNSS (Global Navigation Satellite System) Service (IGS; Beutler *et al.* 1999).

All of these biases are in part responsible for the increased day-to-day scatter in the vertical component of CGPS coordinate solutions and lead to a loss in precision and accuracy. However, as some of these effects have similar magnitudes over large areas, they can often be identified as common mode biases (Wdowinski *et al.* 1997). Hence, by using spatial filtering the common mode can successfully be removed, reducing the day-to-day scatter and improving the error bounds of parameter estimates (e.g. Wdowinski *et al.* 1997; Johansson *et al.* 2002; Nikolaidis 2002; Dong *et al.* 2006). Although, spatial filtering may also de-couple station velocity estimates from the reference frame of the coordinate solutions (Wdowinski *et al.* 1997, 2004).

Besides obtaining highly accurate station velocity estimates, it is essential that a realistic uncertainty is assigned to any estimate. For example, several authors (Langbein & Johnson 1997; Zhang *et al.* 1997; Mao *et al.* 1999; Williams 2003; Williams *et al.* 2004) have shown that CGPS coordinate time-series contain both white and coloured noise, that is, time-independent and time-correlated noise, and if coloured noise is not accounted for station velocity uncertainties may be underestimated by an order of magnitude.

1.2 Aims

Teferle *et al.* (2006) compared the CGPS estimates of vertical land motions obtained for seven CGPS@TG stations to those from AG, geological information, sea level records, and GIA models, and found the CGPS estimates to be offset. Their CGPS estimates were too positive, or less negative, than the other estimates ergo they used a combination of CGPS and AG to align the CGPS estimates to their AG estimates at Newlyn and Lerwick. This study is partly an update of the work of Williams *et al.* (2001) and Teferle *et al.* (2006), but more so an expansion of it in four different ways.

(i) We introduce a second and independent CGPS processing strategy using the Bernese GPS software version 5.0 (Dach *et al.* 2007) in precise point positioning mode (Teferle *et al.* 2007).
(ii) We expand our reference frame implementation from regional (European) to global.
(iii) We include more CGPS stations in Great Britain, to get better coverage.
(iv) We make improvements to the spatial filtering used in Teferle *et al.* (2006) to avoid, as much as possible, a de-coupling of our station velocity estimates from our reference frame implementations.

Through this expansion and the inclusion of more recent data we present the followings:

(i) Updated vertical station velocity estimates from the expanded CGPS network and AG.
(ii) Horizontal station velocity estimates (and residual velocities) for the expanded CGPS network.
(iii) AG-aligned CGPS estimates of vertical crustal motions for the expanded CGPS network, and a comparison of these with estimates from geological information.
(iv) Initial maps of vertical crustal motion for Great Britain based on geodetic data.

The expansion of the CGPS network brought about the inclusion of stations with very different monumentation, often *a priori* deemed inappropriate for geophysical interpretation. Here we follow the approach of previous studies (e.g. Calais *et al.* 2006) and include such stations, then look at their suitability *a posteriori*. In this way, we provide the horizontal and vertical station velocity estimates which form the basis for the studies of Woodworth *et al.* (2009) to update the trends in sea level changes around Great Britain, and of Bradley *et al.* (2009), who investigate the modelling of the GIA processes observed in this region.

1.3 Method

In the following section we discuss the available data sets, that is, from CGPS, AG, and geological information. This is followed by a description of the processing and analysis of the CGPS, AG and geological data before we present our results. For CGPS, we compare our horizontal and vertical station velocity estimates in order to quantify the effects of our two independent CGPS processing strategies, spatial filtering, and reference frame implementations. For AG, we show our best estimates for the change in gravity and derive AG estimates of vertical station velocities from them. The velocity estimates from both geodetic techniques are then interpreted as crustal motions under the assumption that no other local displacement has occurred. For the horizontal component, we then investigate which CGPS stations seem promising for future geophysical interpretations. For the vertical component, we compare our CGPS estimates to those from AG, compute AG-aligned CGPS estimates of vertical crustal motions, and compare these to the latest geological information. Through this process we establish sets of stations for which we have confidence that their station velocity estimates represent present-day crustal motions in Great Britain.

2 DATA SETS

2.1 Continuous GPS

The CGPS stations in Great Britain can be divided into two categories: scientific and network RTK. Data for all of these are archived in the Natural Environment Research Council funded British Isles continuous GNSS Facility (BIGF; http://www.bigf.ac.uk). All of the CGPS stations we considered in this study are shown in Fig. 1.

Four scientific CGPS stations, HERS and HERT at Herstmonceux in southeast England, MORP at Morpeth in northeast England, and

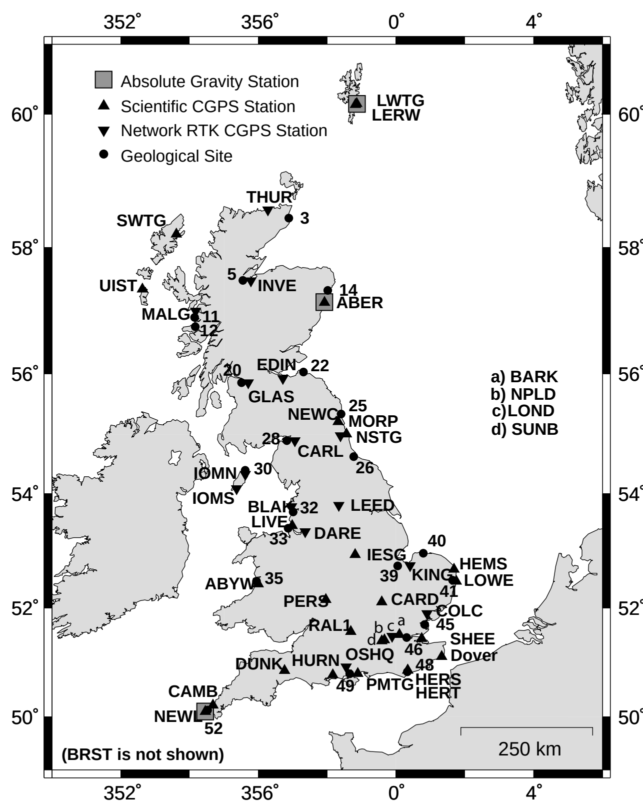

Figure 1. Locations of the scientific CGPS stations, network real-time kinematic (RTK) CGPS stations, absolute gravity (AG) stations, and geological sites (from Shennan & Horton 2002) used in this study.

NPLD at the National Physical Laboratory in Teddington, west of London, contribute to both the IGS and the European Reference Frame Permanent Network (EPN; Bruyninx *et al.* 2001). The scientific CGPS station NEWL in Newlyn, southwest England and ABER in Aberdeen, eastern Scotland, contribute to the IGS TG Benchmark Monitoring (TIGA) Pilot-Project and the European Sea Level Service (ESEAS). NEWL and the two network RTK stations INVE in Inverness, northern Scotland and DARE in Daresbury, northwest England, also contribute to the EPN.

Established in 1992, HERS is the longest operating CGPS station in Great Britain, but its data quality suffered during the 1990s and we regard this station to be of highest quality only after 2001. MORP is certainly an interesting CGPS station within the IGS network due to its unique monumentation, a 4.5 tonne carved monolith that rests directly on top of the underlying bedrock (Blewitt *et al.* 1997). Again, this station suffered from poor data quality in the late 1990s (Teferle 2003), which improved only after modifications in 2002 (IGSMAIL-4222 (2002), see http://igscb.jpl.nasa.gov/mail/igsmail/igsmail.html).

Within BIGF the scientific CGPS stations include those established at ten of the 44 TGs which form the national TG network as part of the National Tidal and Sea Level Facility (http://www.pol.ac.uk/ntslf), 12 others established at sites of the UK Meteorological Office (UKMO) or the Environment Agency (EA), and one at the University of Nottingham. All of these were established during the period from 1997 to 2005 (Table 1).

The CGPS@TG stations have GPS receivers housed in the same building as the TG equipment and the GPS antennas mounted on monuments, sited as close as possible to the TG, i.e. within a few meters of the TG itself; to fulfil the requirement for site-specific, direct estimates of the changes in land level. Teferle (2003) gives further details of these CGPS@TG stations. Due to our interest in sea level studies, we have also included the IGS/EPN station BRST located close to the TG at Brest, France, in our analysis, and we will list it along with the ten CGPS@TG stations located in Great Britain.

The network RTK CGPS stations in Great Britain that are archived in BIGF belong to the Ordnance Survey of Great Britain (OSGB), who have established over 120 such stations since 2000, with larger numbers in more recent years. In this study we only include the 16 stations that were established before 2003 and that have a sufficient and consistent enough data span to warrant any scientific analysis. If they are founded on a stable structure connected to solid rock, then they can provide a series of CGPS stations that densifies the sparse network of scientific stations (Fig. 1 and Table 1).

Overall, we do not consider the CGPS network used in this study as homogeneous. However, we point out elements of homogeneity in the groups of the scientific CGPS stations and the network RTK CGPS stations, which relate to the GPS equipment (Table 1) and the station-specific monumentation (Table 2).

From Table 2 it can be seen that most scientific CGPS stations use IESSG-designed carbon-fibre poles with stainless steel ends that have been attached to either a solid structure or a submerged concrete block that rests directly on top of bedrock, whereas almost all network RTK CGPS stations are located on brick buildings with varying number of storeys. For these stations the monument normally consists of a stainless steel tripod on the roof, or a bracket, which has been mounted on the roof or onto a wall, with the antenna reaching above the roof.

Although HEMS was used for scientific investigations in the past (Teferle *et al.* 2002), the station was decommissioned in 2001 and is mentioned here only for completeness. As DVTG, LWTG, SWTG and UIST were only established in 2005, their coordinate time-series are still too short and we do not discuss these sites further.

2.2 Absolute gravity

AG measurements near TGs began in 1995 at Newlyn and Aberdeen and in 1996 at Lerwick (Williams *et al.* 2001). Given the complexity in making AG measurements we decided to focus our attention on three TG sites. The sites were selected based on their geographical distribution and their representation of the expected changes in land level due to GIA, that is, subsidence at Newlyn in southwest England, uplift or no movement at Aberdeen in eastern Scotland and subsidence at Lerwick on Shetland. Newlyn and Lerwick TGs contribute to the Global Sea Level Observing System (GLOSS) coordinated by the Intergovernmental Oceanographic Commission (IOC) and Newlyn and Aberdeen both have some of the longest and highest quality mean sea level time-series in the country (Williams *et al.* 2001).

At each TG a detailed reconnaissance was carried out to identify potential sites for the establishment of an AG station considered suitable for the long-term monitoring of vertical crustal motion. The main criterion for an AG station is location within a building (for a stable and protected environment) that is likely to have a secure future, with little or no change to its surrounding environment over a sufficient period of time, and built on a bedrock foundation. There are certain effects that restrict the station from being placed at the TG or close to the coastline. The direct gravitational attraction of the ocean mass changes (tidal and non-tidal) close to the TG would impart unwanted noise into the measurements if they are not modelled sufficiently, and it would be difficult to interpret the gravity changes as such. For example, the conversion factor to apply depends on the source of the land movements, that is, free-air for a subsiding pier or Bouguer for a GIA signal. The AG station was, therefore, established sufficiently far from the coastline to minimize these effects while still representing the motion at the TG.

Lerwick AG station is located in the basement of a school, about 0.5 km from the TG and the CGPS@TG station LWTG and 5 km from the scientific CGPS station LERW; Aberdeen AG station is located in a church, about 3.2 km from the TG and the CGPS@TG station ABER; and Newlyn AG station is located in the church at Paul about 1.5 km from the TG and the CGPS@TG station NEWL. We show the locations of AG stations used in this study in Fig. 1.

AG measurements are made by dropping a mass in a vacuum and using an Iodine stabilized He–Ne laser interferometer and rubidium atomic clock to obtain distance–time pairs and solve the equations of motion to obtain the acceleration (Niebauer *et al.* 1995). We use the POL absolute gravimeter (FG5-103), produced commercially by Micro-g LaCoste Inc., USA, to make our measurements. Measurement campaigns at each station are made approximately annually over duration of three to four days. The instrument is set up at the start of each day and the measurements consist of 24 hourly sets of 200 drops spaced 10 s apart. Occasionally, if the measurements do not go as planned, a second trip to the station is organized. Prior to and after each field visit, measurements are made at the gravity station in the laboratory and compared with measurements from our second instrument (FG5-222), to ensure the measurements are consistent. In addition, both instruments are regularly intercompared with other instruments in Europe and the USA to ensure that they are in agreement at the 1–2 μGal level (Williams *et al.* 2001; Vitushkin *et al.* 2002; Francis *et al.* 2005). A summary of the data availability for the AG stations is given in Table 3.

Table 1. Continuous GPS (CGPS) station information for scientific stations co-located with tide gauges (TG), other scientific and network real-time kinematic (RTK) stations in Great Britain used in this study.

Station ID	Domes number	Location	Operator	Longitude (°)	Latitude (°)	Start date	Span (yr)	Current GPS equipment (on 31 December 2005) receiver	Antenna	Radome
					CGPS@TG stations					
ABER	13231M001	Aberdeen	POL[a]/UNT[b]	357.92	57.14	1998-09-18	7.3	ASHTECH Z-XII3	ASH700936F_C	SNOW
BRST	10004M004	Brest, France	IGN[c]	355.50	48.38	1998-10-31	7.2	TRIMBLE 5700	TRM29659.00	NONE
DVTG		Dover	UNT	1.32	51.11	2005-11-24	0.0	ASHTECH UZ-12	ASH701945C_M	SNOW
LIVE	13233M001	Liverpool	UNT	356.98	53.45	1999-02-04	6.9	ASHTECH Z-XII3	ASH700936D_M	SNOW
LOWE	13232M001	Lowestoft	UNT	1.75	52.47	1999-02-13	6.9	ASHTECH Z-XII3	ASH700936F_C	SNOW
LWTG		Lerwick	POL/UNT	358.86	60.15	2005-08-19	0.4	ASHTECH UZ-12	ASH701945C_M	SNOW
NEWL	13273M001	Newlyn	UNT	354.46	50.10	1998-09-30	7.3	ASHTECH Z-XII3	ASH700936D_M	SNOW
NSTG	13216M001	North Shields	NCL[d]/UNT	358.56	55.01	2001-05-15	6.1	ASHTECH Z-XII3	ASH700936B_M	SNOW
PMTG	13289M003	Portsmouth	UNT	358.89	50.80	2001-09-25	4.3	ASHTECH UZ-12	ASH701945C_M	SNOW
SHEE	13236M001	Sheerness	EA[e]/UNT	0.74	51.45	1997-03-26	8.7	TRIMBLE 4000SSI	TRM29659.00	NONE
SWTG		Stornoway	POL/UNT	353.61	58.21	2005-09-02	0.0	ASHTECH UZ-12	ASH701945C_M	SNOW
					Other scientific CGPS stations					
ABYW		Aberystwyth	UKMO[f]	356.00	52.42	1998-04-04	7.7	ASHTECH UZ-12	ASH700936D_M	SNOW
BARK		Barking Barrier	EA/OSGB[g]	0.10	51.52	1997-04-25	8.7	TRIMBLE 4000SSI	TRM29659.00	NONE
CAMB		Camborne	UKMO/OSGB	354.67	50.22	1998-04-03	7.7	ASHTECH UZ-12	ASH700936D_M	SNOW
CARD		Cardington	UKMO	359.58	52.10	2003-01-12	2.9	ASHTECH UZ-12	ASH700936D_M	SNOW
DUNK		Dunkeswell	UKMO	356.76	50.86	2000-02-05	5.9	ASHTECH UZ-12	ASH700936F_C	SNOW
HEMS		Hemsby	UKMO/UNT	1.69	52.69	1998-04-10	2.8	ASHTECH Z-XII3	ASH700936D_M	SNOW
HERS	13212M007	Herstmonceux	NSGF[h]	0.34	50.87	1992-03-24	8.7	ASHTECH Z-XII3	ASH700936E	NONE
HERT	13212M010	Herstmonceux	NSGF	0.33	50.87	2003-03-12	2.8	ASHTECH Z18	ASH701946.2	NONE
HURN		Hurn	UKMO/UNT	358.16	50.78	2000-09-13	5.3	ASHTECH Z-XII3	ASH700936F_C	SNOW
IESG	13220M001	Nottingham	UNT	358.81	52.94	1997-04-27	8.7	ASHTECH Z-XII3	ASH700936D_M	SNOW
LERW		Lerwick	UKMO/OSGB	358.82	60.14	1998-04-18	7.7	ASHTECH Z-XII3	ASH700936D_M	SNOW
MORP	13299S001	Morpeth	NCL	358.31	55.21	1996-10-31	8.7	ASHTECH Z-XII3	AOAD/M_T	NONE
NPLD	13234M003	Teddington	NPL[i]	359.66	51.42	2000-08-16	4.9	ASHTECH Z-XII3T	AOAD/M_T	NONE
PERS		Pershore	UKMO/UNT	357.96	52.15	2001-05-09	4.6	ASHTECH Z-XII3	ASH700936F_C	SNOW
RAL1		Chilton	UKMO	358.69	51.57	2003-03-11	2.8	ASHTECH UZ-12	ASH700936F_C	SNOW
SUNB		Sunbury Yard	EA/UNT	359.58	51.40	1997-04-08	8.7	TRIMBLE 4000SSI	TRM29659.00	NONE
UIST		Uist	UKMO	352.63	57.35	2005-01-21	0.9	ASHTECH UZ-12	ASH700936D_M	SNOW
					Network RTK CGPS stations					
BLAK		Blackpool	OSGB	356.97	53.78	2002-01-02	4.0	LEICA RS500	LEIAT504	LEIS
CARL	13205S001	Carlisle	OSGB	357.06	54.90	2000-04-12	5.7	LEICA RS500	LEIAT504	LEIS
COLC	13207S001	Colchester	OSGB	0.90	51.89	2000-04-27	5.7	LEICA RS500	LEIAT504	LEIS
DARE	13208S001	Daresbury	OSGB	357.36	53.34	2001-12-03	5.7	LEICA RS500	LEIAT504	LEIS
EDIN	13217S001	Edinburgh	OSGB	356.71	55.92	2000-03-16	5.8	LEICA RS500	LEIAT504	LEIS
GLAS	13219S001	Glasgow	OSGB	355.70	55.85	2000-03-15	5.8	LEICA RS500	LEIAT504	LEIS
INVE	13221S001	Inverness	OSGB	355.78	57.49	2002-07-05	6.0	LEICA SR530	ASH700936E	SNOW
IOMN	13222S001	Ramsay	OSGB	355.61	54.33	2001-03-21	4.8	LEICA RS500	LEIAT504	LEIS
IOMS	13224S001	Ronaldsway	OSGB	355.37	54.09	2001-03-20	4.8	LEICA RS500	LEIAT504	LEIS
KING	13225S001	King’s Lynn	OSGB	0.40	52.75	2000-01-02	6.0	LEICA SR530	ASH700936E	SNOW
LEED	13215S001	Leeds	OSGB	358.34	53.80	2000-01-02	6.0	LEICA SR530	ASH700936E	SNOW
LOND		London	OSGB	359.88	51.49	2000-01-02	6.0	LEICA SR530	ASH700936E	SNOW
MALG	13226S001	Mallaig	OSGB	354.17	57.01	2000-05-31	5.6	LEICA RS500	LEIAT504	LEIS
NEWC	13227S001	Newcastle	OSGB	358.38	54.98	2000-01-02	6.0	LEICA SR530	ASH700936E	SNOW
OSHQ	13274S002	Southampton	OSGB	358.55	50.93	2000-01-02	6.0	LEICA SR530	ASH700936E	SNOW
THUR	13230S001	Thurso	OSGB	356.27	58.58	2000-05-09	5.6	LEICA RS500	LEIAT504	LEIS

Notes: Start date either depicts the point in time of the actual station installation or for some sites, the point in time from which data is available from in the British Isles continuous GNSS Facility (BIGF). Span depicts the maximum theoretical period for which data were available in the archive up to 2005 December 31.

[a]Proudman Oceanographic Laboratory (POL).
[b]University of Nottingham (UNT).
[c]Institut Géographique National (IGN).
[d]Newcastle University (NCL).
[e]Environment Agency (EA).
[f]United Kingdom Meteorological Office (UKMO).
[g]Ordnance Survey of Great Britain (OSGB).
[h]National Space Geodetic Facility (NGSF).
[i]National Physical Laboratory (NPL).

Table 2. Monumentation information for CGPS stations in Great Britain used in this study.

Station ID	Domes	Location	Monumentation Information
			CGPS@TG stations
ABER	13231M001	Aberdeen	4 m high c/f pipe attached to s/s plate connected to concrete quay with piled foundations
BRST	10004M004	Brest, France	2 m high s/s mast connected to stone pier
DVTG		Dover	2 m high c/f pipe attached to s/s plate connected to stone pier
LIVE	13233M001	Liverpool	5 m high concrete pillar connected to stone pier with piled foundations
LOWE	13232M001	Lowestoft	0.8 m high c/f pipe attached to s/s bracket connected to side wall of 2-storey building on concrete quay with piled foundations
LWTG		Lerwick	3 m high c/f pipe attached to s/s plate connected to stone pier
NEWL	13273M001	Newlyn	3 m high c/f pipe attached to s/s plate connected to observation platform of steel lighthouse on stone pier
NSTG	13216M001	North Shields	4 m high aluminium pole connected to concrete quay with piled foundations
PMTG	13289M003	Portsmouth	1.5 m high s/s pole and bracket connected to side wall of 1-storey building on stone quay
SHEE	13236M001	Sheerness	0.2 m high s/s bracket connected to flat roof of 1-storey building on concrete jetty with piled foundations
SWTG		Stornoway	2 m high c/f pipe attached to s/s plate connected to concrete wharf with piled foundations
			Other scientific CGPS stations
ABYW		Aberystwyth	2 m high c/f pipe attached to s/s plate connected to ∼3 m deep concrete block founded on bedrock
BARK		Barking Barrier	0.6 m high s/s pole and bracket connected to ∼40 m high concrete structure founded on bedrock
CAMB		Camborne	2 m high c/f pipe attached to s/s plate connected to ∼2 m deep concrete block founded on bedrock
CARD		Cardington	2 m high c/f pipe attached to s/s plate connected to ∼1 m deep concrete block
DUNK		Dunkeswell	2 m high c/f pipe attached to s/s plate connected to ∼2 m deep concrete block founded on bedrock
HEMS		Hemsby	2 m high c/f pipe attached to s/s plate connected to flat roof of 1-storey building with piled foundations
HERS	13212M007	Herstmonceux	8 m high steel mast connected to ∼5 m deep concrete block
HERT	13212M010	Herstmonceux	0.5 m high brick/concrete pillar on top of water tower with ∼5 m deep foundations
HURN		Hurn	2 m high c/f pipe attached to s/s plate connected to ∼1 m deep concrete block
IESG	13220M001	Nottingham	0.6 m high s/s pole and bracket connected to ∼13 m high brick turret founded on bedrock
LERW		Lerwick	2 m high c/f pipe attached to s/s plate connected to ∼1 m deep concrete block founded on bedrock
MORP	13299S001	Morpeth	2.4 m high, 4.5 tonne quarried trapezoidial stone buried to ∼2.4 m depth and founded on bedrock
NPLD	13234M003	Teddington	On roof of multistorey building
PERS		Pershore	2 m high c/f pipe attached to s/s plate connected to ∼1 m deep concrete block
RAL1		Chilton	On roof of multi-storey building
SUNB		Sunbury Yard	0.6 m high c/f pipe attached to s/s bracket connected to side wall of 2-storey building
UIST		Uist	2 m high c/f pipe attached to s/s plate connected to ∼1 m deep concrete block
			Network RTK CGPS stations
BLAK		Blackpool	∼2 m high s/s pole connected to side wall of 1-storey brick building (∼4 m tall)
CARL	13205S001	Carlisle	∼1.8 m high s/s tripod connected to roof of 3-storey concrete building (∼9 m tall)
COLC	13207S001	Colchester	∼2 m high s/s pole connected to side wall of multi-storey brick and concrete building (∼22 m tall)
DARE	13208S001	Daresbury	∼2 m high s/s pole connected to side wall of 1-storey brick building (∼5 m tall)
EDIN	13217S001	Edinburgh	∼2 m high s/s pole connected to side wall of 1-storey brick building (∼5 m tall)

Table 2. (*Continued.*)

Station ID	Domes	Location	Monumentation Information
GLAS	13219S001	Glasgow	∼2 m high s/s pole connected to side wall of 2-storey brick building (∼6 m tall)
INVE	13221S001	Inverness	∼2 m high s/s pole connected to side wall of 2-storey block building (∼8 m tall)
IOMN	13222S001	Ramsay	no information available
IOMS	13224S001	Ronaldsway	no information available
KING	13225S001	King's Lynn	∼1.8 m high steel tripod connected to flat roof of multi-storey brick building (∼13 m tall)
LEED	13215S001	Leeds	∼1.8 m high steel tripod connected to flat roof of 3-storey building (∼13 m tall)
LOND		London	∼1.8 m high steel tripod connected to roof of multi-storey building
MALG	13226S001	Mallaig	∼2 m high s/s pole connected to side wall of 2-storey brick building (∼7 m tall)
NEWC	13227S001	Newcastle	∼1.8 m high steel tripod connected to concrete block on flat roof of 4-storey brick building (∼12 m tall)
OSHQ	13274S002	Southampton	∼1.8 m high s/s tripod connected to flat roof of multi-storey re-inforced concrete building (∼24 m tall)
THUR	13230S001	Thurso	∼3 m high steel mast connected to flat roof of 2-storey concrete building (∼6 m tall)

Notes: Information is given for scientific stations colocated with tide gauges (TG), other scientific, and network real-time kinematic (RTK) stations and was accurate as of 2005 December 31. c/f stands for carbon-fibre and s/s for stainless steel.

Table 3. Data availability for the absolute gravity (AG) stations in Great Britain used in this study.

Station	Start date	End date	# of campaigns	Data span
Lerwick	1996-09	2006-08	10	9.9
Aberdeen	1995-05	2006-08	13	11.3
Newlyn	1995-10	2006-09	12	10.9

2.3 Geological information

The database of Holocene sea level index points held at Durham University (Shennan 1989; Shennan & Horton 2002; Shennan *et al.* 2006) allows investigations of Holocene, and ongoing, land and sea level changes in Great Britain. Observations, with quantified uncertainty terms, of past changes in sea level relative to present come from sediments, both organic and minerogenic, and from morphological features whose origin was controlled by palaeo-sea level. In order to be useful, sediments must not have been eroded or transported since the time of accumulation and where such sediments and morphological features survive, they can be used as sea level index points by defining attributes such as location, age, altitude and tendency (Shennan *et al.* 2006). If no transportation of the sediments can be assumed, then the location attribute of a sea level index point is defined by its geographical coordinates. The age attribute is obtained from radiocarbon techniques with calibrated ages as 95 per cent confidence limits using Calib 4.4 (http://depts.washington.edu/qil). We wish to mention that most sea level index points in the database from Great Britain have at least one type of corroborating evidence to support the radiocarbon age and to demonstrate continuity of sedimentation. The ages of most sea level index points range between 3000 and 10 000 calibrated years before present (cal. yr BP), with some sites in northwest Scotland having the longest records dating back to up to 15 000 cal. yr BP. With very few locations worldwide providing such long (>10 000 year) records of relative sea level change, these are key to determining changes in global ice volume (Shennan *et al.* 2006). We show the sea level index points from Shennan & Horton (2002) used in this study in Fig. 1 and list associated information in Table 4.

3 PROCESSING AND ANALYSIS

3.1 Continuous GPS

We utilized two independent CGPS processing strategies during our analysis of the daily GPS observation data from Great Britain and our reference frame networks. Following the examples of Geirsson *et al.* (2006) and Kierulf *et al.* (2008), by having multiple independent solutions (softwares/strategies) we are able to better understand processing strategy specific issues which may be of station-specific or solution-specific character. As we will show, at this stage it is important for the investigations to be carried out separately as the specific effects may be diluted by a combination process.

In the first strategy, we used the IESSG's GPS Analysis Software version 2.4 (GAS2.4; Stewart *et al.* 2002) to produce a series of daily double-difference (DD) regional network (RN) solutions (Teferle 2003; Teferle *et al.* 2006), below denoted as DDRN, for the period from 1997 March to 2005 December. In this case, the reference frame definition was effected through the inclusion of four European IGS stations, with well-determined station coordinates and velocities in the ITRF2000, as reference stations (Fig. 2).

In the second strategy, we used the IESSG's GNSS processing tools to run the Bernese software version 5.0 (BSW5.0; Dach *et al.* 2007) to produce a series of daily precise point positioning (PPP) globally transformed (GT) solutions (Teferle *et al.* 2007), below denoted as PPPGT, for the period from 2000 January to 2005 December. In this case, the reference frame definition was effected by using the 99 IGS reference frame stations included in IGb00 [IGSMAIL-4748 (2003); IGSMAIL-4928 (2004) on http://igscb.jpl.nasa.gov/mail/igsmail/igsmail.html], the IGS realization of ITRF2000, as reference stations when computing the transformation parameters (Fig. 2).

After the CGPS processing, we formed coordinate time-series in ITRF2000 from the daily position solutions from both processing

Table 4. Information on sites with geological evidence for vertical crustal motions in Great Britain from Shennan & Horton (2002).

Site number	Site name	Lon (°)	Lat (°)	Rate (mm yr^{-1})	CGPS station	Distance (km)
3	Wick	356.88	58.45	0.42	THUR	38
5	Moray Firth	355.54	57.49	1.11	INVE	14
14	Aberdeen	358.01	57.33	0.69	ABER	21
11	NW Scotland (Arisaig)	354.15	56.91	1.01	MALG	11
	NW Scotland (Kentra)	354.16	56.76	1.00	MALG	28
22	SE Scotland	357.31	56.03	1.15	EDIN	39
20	Clyde	355.51	55.86	1.53	GLAS	12
28	South Solway Firth	356.83	54.90	0.87	CARL	15
30	Isle of Man	355.61	54.40	0.45	IOMN	7
					IOMS	38
25	NE England (South)	358.40	55.34	0.17	MORP	15
					NEWC	40
					NSTG	38
26	Tees	358.77	54.63	−0.17	NEWC	46
					NSTG	44
32	Lancashire	357.01	53.69	0.47	BLAK	11
					LIVE	26
33	Mersey	356.86	53.40	−0.21	DARE	34
					LIVE	10
35	Mid Wales	355.94	52.47	−0.38	ABYW	7
39	Fens	0.04	52.74	−0.37	KING	24
40	Norfolk	0.79	52.97	−0.60	KING	35
41	East Anglia	1.64	52.49	−0.60	LOWE	7
45	Essex	0.83	51.70	−0.85	SHEE	28
					COLC	23
46	Thames	0.31	51.46	−0.74	BARK	16
					SHEE	30
48	Sussex	0.33	50.84	−0.42	HERS	3
					HERT	3
49	Hampshire	358.65	50.80	−0.58	PMTG	17
					OSHQ	17
52	SW England (Cornwall)	354.52	50.13	−1.12	CAMB	15
					NEWL	5

Notes: Site number and name are given as published, the rate is the best estimate from Shennan & Horton (2002) and each site has been assigned CGPS stations close-by, with distance given.

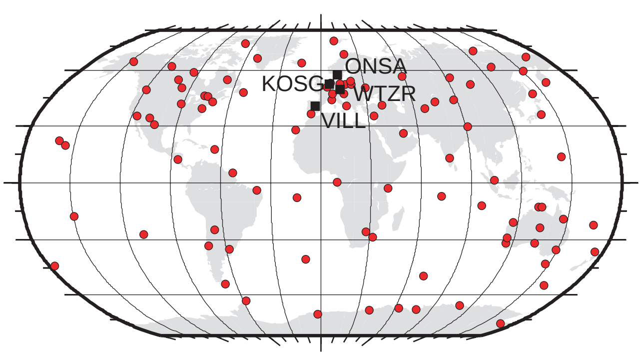

Figure 2. Reference frame stations used by the GAS2.4 DD regional network (squares) and the BSW5.0 globally transformed PPP (circles) solutions.

strategies for each of the CGPS stations. As such daily coordinate estimates have been shown to contain both temporal (e.g. Zhang *et al.* 1997; Mao *et al.* 1999; Williams 2003; Williams *et al.* 2004) and spatial (e.g. Wdowinski *et al.* 1997; Nikolaidis 2002; Dong *et al.* 2006) correlations we apply the following coordinate time-series analysis strategy.

To account for white and coloured noise (temporally correlated errors) in our coordinate time-series, we estimate, using the coordinate time-series analysis software CATS (Williams 2008) which employs Maximum-Likelihood estimation (MLE), the parameters of a linear velocity, annual and semi-annual periodic terms, coordinate offset magnitudes, and the noise amplitudes for both white and coloured noise components. For the coloured noise component we choose flicker noise rather than another power-law process, as it has been shown to be widely present and a very appropriate model in CGPS coordinate time-series (Williams *et al.* 2004).

We use spatial filtering to reduce the spatially correlated features within the coordinate time-series, to improve the signal-to-noise ratio and station velocity uncertainties. Several spatial filtering methods involving simple unweighted and weighted stacking of daily residuals (e.g. Wdowinski *et al.* 1997; Nikolaidis 2002; Wdowinski *et al.* 2004) to more complex methods using Empirical Orthogonal Functions (Dong *et al.* 2006; Teferle *et al.* 2008) have been suggested. Following Teferle *et al.* (2006), we use the weighted stacking method to compute the daily common mode bias as the weighted mean coordinate residual from a selection of stations on a particular day and subtract this bias estimate from all unfiltered coordinate time-series, forming our filtered coordinate time-series.

It has been suggested that the coordinate time-series used for the computation of the common mode bias should be of high quality and not show any station-specific features (e.g. Wdowinski *et al.* 1997; Nikolaidis 2002; Teferle 2003). This ensures that the computed bias only contains the common systematic variations of the coordinate time-series for a particular solution, as including a CGPS station behaving in an unusual manner, that is, due to large multipath or interference effects, would change the common mode estimate.

We argue that the effect of spatial filtering should merely be an improvement in the signal-to-noise ratio of the coordinate time-series and should not affect station velocity estimates such that a departure, that is, a de-coupling, from a given reference frame occurs (Wdowinski *et al.* 1997, 2004).

In previous studies (e.g. Nikolaidis 2002; Wdowinski *et al.* 1997, 2004), annual and semi-annual signals in the coordinate time-series were assumed to be part of the spatially correlated noise and hence were not modelled during the common mode bias computation, giving very smooth filtered coordinate time-series. Only Prawirodirdjo *et al.* (2006) argued to model both these signals when computing the daily common mode bias in order for the common mode to contain only noise and not predictable thermo-elastic signal.

It is also well known that annual and semi-annual signals in coordinate time-series can significantly bias station velocity estimates (Blewitt & Lavallée 2002). Assuming typical amplitudes of 2–4 and 1–2 mm for annual and semi-annual signals, Blewitt & Lavallée (2002) recommended that coordinate time-series with data time spans of less than 2.5 yr should not be considered for investigations and that for those with more than 2.5 yr the additional estimation of annual and semi-annual periodic terms would avoid the associated velocity bias. Furthermore, they stated that this simultaneous estimation may not be necessary, once time-series reached a span of more than 4.5 yr. With amplitudes of these signals often being significantly larger, it seems beneficial to continue to model these signals. Therefore, we argue that not including terms for these signals during the common mode bias computation may lead to a non-zero, artificial linear trend in the daily common mode bias time-series itself, which in turn will alter the trend of the filtered coordinate time-series thereby biasing station velocity estimates. Although we agree that as the velocity bias due to periodic signals reduces with increasing length of the time-series, this issue will become less prominent for spatial filtering of longer ones.

Another factor that can influence station velocity estimates of filtered coordinate time-series that has, so far, not been mentioned in the published literature and may thus be easily overlooked, is related to the way the station velocities are estimated in the common mode bias computation and thereafter in the analysis of the filtered coordinate time-series. Already Zhang *et al.* (1997) reported millimetre-level differences in their velocity estimates between those obtained from weighted least squares and more complex MLE. Similar differences between the two methods for computing station velocities were also reported in Teferle (2003) for some of the CGPS stations used in this study. As the station velocities are estimated several times during spatial filtering and the following analysis, it might seem convenient to mix both methods for computational efficiency and a faster analysis. Considering the above reported velocity differences, we argue that mixing of both methods potentially introduces a velocity bias. In order to avoid this bias, we consistently use MLE throughout the common mode bias estimation and the following analysis of the filtered coordinate time-series.

3.2 Absolute gravity

The processing and analysis of the AG measurements was carried out using the GAP (Gravity@POL) software developed at POL. The data from each drop were fit using least squares to an equation of motion that includes a known a-priori vertical gravity gradient. The measurements of time were also corrected for the time delay due to the finite speed of light. The gravity gradients for Newlyn and Aberdeen have been measured using a relative spring gravimeter (Hopewell 2003). For Lerwick, a standard value equal to the free-air correction of $-0.3086\ \mu\mathrm{Gal\ mm}^{-1}$ was used. Standard corrections were made for solid Earth tides, ocean tide loading, polar motion, and comparator response (Niebauer *et al.* 1995; Williams *et al.* 2001). Geophysical corrections were made for atmospheric loading using a single admittance factor and local pressure data. No attempt was made to correct for hydrological loading. Finally, the results were transferred from the height of observation to a common reference height. Data from each day were then combined into a single mean value. To estimate the AG rates and their uncertainties we used weighted least squares and assumed the gravity noise budget consisted of an instrumental set up error (1.6 μGal; Van Camp *et al.* 2005) that was common to all days during the measurement campaign, a statistical error based on the daily drop-to-drop standard deviations, and a long period noise that was modelled as a first-order Gauss Markov process (Van Camp *et al.* 2005). In an additional step, the error bars for each measurement campaign are scaled by the reduced chi-square fit to the mean value over those days in an attempt to reflect the short-term day-to-day scatter.

To obtain an estimate of the vertical station velocity and associated uncertainty we need to apply a gravity/uplift ratio. This ratio is dependent on many factors, not least the physical processes causing the deformation. Estimates from various models range from $-0.15\ \mu\mathrm{Gal\ mm}^{-1}$ (Wahr *et al.* 1995) to $-0.26\ \mu\mathrm{Gal\ mm}^{-1}$ (de Linage *et al.* 2007). Computed ratios from data range from $-0.18 \pm 0.03\ \mu\mathrm{Gal\ mm}^{-1}$ (Lambert *et al.* 2006) through $-0.20 \pm 0.06\ \mu\mathrm{Gal\ mm}^{-1}$ to $-0.24 \pm 0.13\ \mu\mathrm{Gal\ mm}^{-1}$ (Mazzotti *et al.* 2007). We used a gravity/uplift ratio of $-0.2\ \mu\mathrm{Gal\ mm}^{-1}$ or $-5\ \mathrm{mm}\ \mu\mathrm{Gal}^{-1}$ which is the mean of all these estimates. We do not, as yet, propagate uncertainties of the ratio, into the vertical station velocities. Neither are we prepared, given the scale of the deformation expected in Great Britain compared to Fennoscandia or North America, to attempt to estimate a ratio from the GPS and AG data sets.

3.3 Geological information

We obtain an estimate of relative vertical crustal motion from the geological information by fitting a linear trend to relative sea level data from as early as 4000 cal. yr BP to the present day (Shennan 1989; Shennan & Horton 2002). In some cases the oldest data are younger than 4000 cal. yr BP and so the regression is over a shorter and more recent period. In applying this procedure, we assume that there has been a negligible secular height shift of the sea surface over the period for which data exist at a given locality. Specifically, we have assumed that there is no significant ocean surface height change due to contemporaneous mass changes in continental ice sheets and glaciers or due to ocean water density changes.

GIA can lead to ocean surface height changes in the UK through two processes. One is regional perturbations to the gravity field due to vertical land motion. The corresponding geoid height shift is spatially correlated with the land motion signal, but is more than an order of magnitude smaller (i.e. $<0.1\ \mathrm{mm\ yr}^{-1}$ at most sites) and so is not accounted for here. A second process that leads to a global-scale lowering of the ocean surface following the last glacial maximum is known as ocean siphoning (Mitrovica & Peltier 1991; Mitrovica & Milne 2002). This process is due to increasing ocean basin volume associated with vertical motion of the ocean

Table 5. GPS results related acronyms and definitions used throughout this study.

Acronym	Definition
GAS2.4	GPS Analysis Software Version 2.4
BSW5.0	Bernese GPS Software Version 5.0
DD	Double-difference
DDRN	GAS2.4 double-difference regional network
DDRNU	Unfiltered GAS2.4 DD regional network coordinate time-series
DDRNF	Filtered GAS2.4 DD regional network coordinate time-series
PPP	Precise point positioning
PPPGT	BSW5.0 globally transformed precise point positioning
PPPGTU	Unfiltered BSW5.0 globally transformed PPP coordinate time-series
PPPGTF	Filtered BSW5.0 globally transformed PPP coordinate time-series

floor. Current GIA models predict this lowering to be about 0.2–0.4 mm yr^{-1} during the late Holocene (e.g. Peltier 2001) and so estimates of vertical crustal motions inferred from relative sea level data will be biased high (i.e. more positive) by this amount. Since the magnitude of this effect is relatively small, we do not explicitly revise the values of vertical crustal motion estimated from the relative sea level data. However, in the data comparisons that follow, we are mindful that the inferred estimates have a positive bias by a few tenths of a millimetres per year.

4 RESULTS

This section presents the horizontal and vertical station velocity estimates from CGPS. Using these estimates we carry out comparisons to quantify the effects of the two independent CGPS processing strategies, spatial filtering, and reference frame implementations. Following this we present the vertical station velocity estimates from AG and the geological information before we start the interpretation of the station velocity estimates as crustal motions. Based on our horizontal station velocity estimates we investigate the suitability of the current CGPS network to provide estimates of horizontal crustal motion for geophysical interpretations, i.e. plate motions or on a more demanding scale, the motions associated with GIA processes. Using the vertical station velocity estimates we carry out a comparison of these to those from AG, compute AG-aligned CGPS vertical station velocities, and compare these to vertical crustal motions from the geological evidence.

For convenience, we list the definitions of relevant acronyms which will be used extensively in the following sections in Table 5.

4.1 Continuous GPS

We used the daily coordinate estimates for both CGPS processing strategies to form coordinate time-series for 39 of the 44 CGPS stations in Table 1. As outlined above, we used spatial filtering based on weighted stacking to obtain filtered coordinate time-series for both independent CGPS processing strategies.[1] In this manner, we arrived at four different solutions, namely the unfiltered and filtered GAS2.4 DD regional network coordinate time-series solutions, below denoted as solutions DDRNU and DDRNF, and the unfiltered and filtered BSW5.0 globally transformed PPP coordinate time-series solutions, below denoted as solutions PPPGTU and PPPGTF.

All four solutions use data for the period up to 2005 December 31, but differ in their time span as outlined previously. For solutions

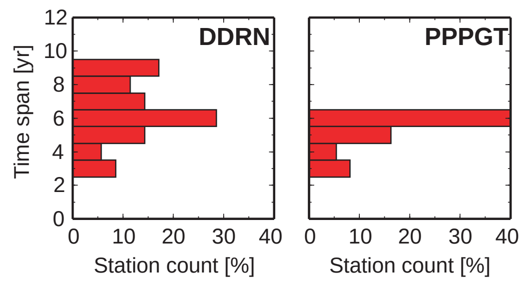

Figure 3. Distribution of coordinate time-series lengths for the GAS2.4 DD regional network (DDRN) and BSW5.0 globally transformed PPP (PPPGT) solutions.

PPPGTU and PPPGTF we considered the currently available satellite orbit and clock products to be of not good enough quality prior to 2000 (Teferle *et al.* 2007). From Fig. 3, it is clear that over 70 per cent of our coordinate time-series span a period of more than 5 yr.

We show the unfiltered and spatially filtered coordinate time-series for each CGPS station for solutions DDRNU, DDRNF, PPPGTU and PPPGTF, respectively, in Figs S1–S4 of the Supporting Information.

4.1.1 Horizontal station velocities

We obtained horizontal station velocity estimates and associated uncertainties from the MLE for all four coordinate time-series solutions (Table 6 and Table S1 of the Supporting Information).

In the case of solutions DDRNU and DDRNF we excluded BLAK, COLC, HERT, LOND and OSHQ due to network size limitations in the GAS2.4 software while for the solutions PPPGTU and PPPGTF, BRST and RAL1 gave unreasonably noisy daily coordinate estimates. HEMS was excluded due to its short data span, as it was decommissioned in 2001.

We draw several general conclusions from Table 6. First of all, the four solutions show excellent overall agreement in their velocity estimates, well within their uncertainties (all uncertainties here and throughout this study are 1σ). Second, there is a reduction in the range of the velocity uncertainties for solutions DDRNF and PPPGTF compared to those of solutions DDRNU and PPPGTU, respectively, which is a first indication of the effectiveness of the spatial filter.

To investigate the effect of the CGPS processing strategy on the horizontal velocities we computed the mean of the velocity differences (and their corresponding standard deviations) between solutions DDRNU and PPPGTU to be -0.0 ± 0.4 and 0.1 ± 0.7 mm yr^{-1}, for north and east, respectively. Similarly, we computed the mean of the velocity differences (and their corresponding

[1] Details on the particular implementation of spatial filtering can be found in Appendix A.

Table 6. CGPS horizontal station velocity estimates for unfiltered GAS2.4 DD regional network (DDRNU), unfiltered BSW5.0 globally transformed PPP (PPPGTU), filtered GAS2.4 DD regional network (DDRNF) and filtered BSW5.0 globally transformed PPP (PPPGTF) coordinate time-series solutions. All values are in mm yr^{-1}. Uncertainties are 1σ.

	DDRNU		PPPGTU		DDRNF		PPPGTF	
	North (mm yr^{-1})	East (mm yr^{-1})	North (mm yr^{-1})	East (mm yr^{-1})	North (mm yr^{-1})	East (mm yr^{-1})	North (mm yr^{-1})	East (mm yr^{-1})
				CGPS@TG stations				
ABER	14.7 ± 0.3	15.3 ± 0.6	14.9 ± 0.3	15.1 ± 0.5	14.7 ± 0.2	15.1 ± 0.3	14.6 ± 0.2	15.4 ± 0.3
BRST	16.0 ± 0.4	17.6 ± 0.7	n/a	n/a	16.0 ± 0.4	17.7 ± 0.6	n/a	n/a
LIVE	13.6 ± 0.4	17.3 ± 0.7	13.3 ± 0.5	16.8 ± 0.7	13.5 ± 0.3	17.1 ± 0.3	13.3 ± 0.4	16.8 ± 0.3
LOWE	14.8 ± 0.2	18.4 ± 0.4	15.0 ± 0.2	18.0 ± 0.4	14.9 ± 0.2	18.6 ± 0.3	15.0 ± 0.1	18.0 ± 0.2
NEWL	16.1 ± 0.3	16.7 ± 0.5	15.7 ± 0.3	16.5 ± 0.4	16.0 ± 0.2	16.7 ± 0.4	15.7 ± 0.2	16.5 ± 0.2
NSTG	14.5 ± 0.3	17.3 ± 0.7	15.2 ± 0.4	16.3 ± 0.6	14.7 ± 0.2	17.4 ± 0.6	15.1 ± 0.2	16.3 ± 0.5
PMTG	17.4 ± 0.6	19.6 ± 0.6	16.1 ± 0.5	19.2 ± 0.5	17.5 ± 0.5	20.5 ± 0.4	16.3 ± 0.4	19.5 ± 0.3
SHEE	15.3 ± 0.3	18.0 ± 0.4	14.9 ± 0.4	17.1 ± 0.5	15.4 ± 0.3	17.9 ± 0.2	14.9 ± 0.4	17.1 ± 0.3
				Other scientific CGPS stations				
ABYW	15.9 ± 0.2	17.9 ± 0.5	15.9 ± 0.3	17.2 ± 0.4	16.0 ± 0.1	17.8 ± 0.3	15.9 ± 0.1	17.1 ± 0.2
BARK	15.3 ± 0.5	17.7 ± 0.4	15.5 ± 0.6	16.8 ± 0.6	15.3 ± 0.5	17.7 ± 0.4	15.6 ± 0.6	16.9 ± 0.4
CAMB	16.0 ± 0.3	17.3 ± 0.5	15.9 ± 0.3	16.7 ± 0.4	15.9 ± 0.2	17.3 ± 0.2	15.8 ± 0.1	16.5 ± 0.2
CARD	15.4 ± 0.5	16.7 ± 1.0	16.1 ± 1.0	18.0 ± 2.4	15.6 ± 0.3	18.0 ± 0.6	14.7 ± 0.9	17.9 ± 2.1
DUNK	15.7 ± 0.6	17.4 ± 0.7	15.5 ± 0.3	17.3 ± 0.5	15.7 ± 0.4	17.9 ± 0.4	15.5 ± 0.1	17.1 ± 0.2
HEMS	14.3 ± 0.8	20.4 ± 1.0	n/a	n/a	14.2 ± 0.6	19.5 ± 0.6	n/a	n/a
HERS	14.4 ± 0.4	17.9 ± 0.6	15.0 ± 0.4	17.2 ± 0.6	14.4 ± 0.3	18.0 ± 0.5	15.0 ± 0.3	17.1 ± 0.3
HERT	n/a	n/a	14.9 ± 0.6	16.4 ± 1.1	n/a	n/a	14.8 ± 0.4	16.5 ± 0.9
HURN	14.8 ± 0.4	17.0 ± 0.9	14.6 ± 0.3	17.1 ± 0.4	15.1 ± 0.3	17.1 ± 0.3	14.3 ± 0.2	17.3 ± 0.1
IESG	14.5 ± 0.2	17.7 ± 0.3	14.8 ± 0.2	17.0 ± 0.4	14.5 ± 0.1	17.7 ± 0.2	14.8 ± 0.1	17.0 ± 0.1
LERW	16.0 ± 0.3	13.7 ± 0.6	16.0 ± 0.3	13.7 ± 0.3	16.0 ± 0.2	13.7 ± 0.3	15.9 ± 0.2	13.6 ± 0.2
MORP	16.1 ± 0.4	14.6 ± 0.6	16.5 ± 0.9	16.4 ± 1.1	16.0 ± 0.4	14.4 ± 0.5	16.7 ± 0.8	16.7 ± 0.9
NPLD	15.1 ± 0.4	17.2 ± 0.5	14.9 ± 0.4	17.0 ± 0.5	15.0 ± 0.2	17.2 ± 0.4	14.6 ± 0.2	17.0 ± 0.3
PERS	15.4 ± 0.3	16.0 ± 0.5	15.7 ± 0.4	15.8 ± 0.6	15.5 ± 0.1	16.6 ± 0.3	15.4 ± 0.2	16.0 ± 0.4
RAL1	15.0 ± 0.5	17.0 ± 0.7	n/a	n/a	15.2 ± 0.1	17.8 ± 0.4	n/a	n/a
SUNB	15.4 ± 0.3	18.1 ± 0.6	15.5 ± 0.4	16.6 ± 0.5	15.4 ± 0.2	18.1 ± 0.5	15.4 ± 0.3	16.5 ± 0.4
				Network RTK CGPS stations				
BLAK	n/a	n/a	15.1 ± 0.4	16.6 ± 0.5	n/a	n/a	15.0 ± 0.2	16.4 ± 0.2
CARL	15.1 ± 0.4	15.5 ± 0.6	15.1 ± 0.3	15.8 ± 0.4	15.2 ± 0.1	16.2 ± 0.2	15.2 ± 0.1	15.9 ± 0.1
COLC	n/a	n/a	15.4 ± 0.3	17.3 ± 0.4	n/a	n/a	15.4 ± 0.1	17.6 ± 0.2
DARE	15.6 ± 0.3	16.5 ± 0.6	15.5 ± 0.3	16.5 ± 0.4	15.7 ± 0.1	16.8 ± 0.2	15.7 ± 0.1	16.4 ± 0.1
EDIN	15.4 ± 0.4	15.4 ± 0.6	15.3 ± 0.3	15.2 ± 0.4	15.4 ± 0.3	15.8 ± 0.2	15.5 ± 0.1	15.3 ± 0.1
GLAS	15.8 ± 0.3	14.3 ± 0.6	15.6 ± 0.3	14.9 ± 0.4	15.8 ± 0.2	14.8 ± 0.3	15.8 ± 0.1	14.9 ± 0.2
INVE	15.4 ± 0.4	15.7 ± 0.7	15.6 ± 0.3	15.1 ± 0.4	15.4 ± 0.3	15.7 ± 0.4	15.5 ± 0.1	15.2 ± 0.3
IOMN	15.2 ± 0.6	14.7 ± 0.8	15.6 ± 0.5	15.6 ± 0.5	15.1 ± 0.6	15.8 ± 0.4	15.3 ± 0.4	15.6 ± 0.2
IOMS	15.6 ± 0.4	14.4 ± 0.7	15.7 ± 0.3	15.7 ± 0.5	15.6 ± 0.3	15.8 ± 0.2	15.5 ± 0.1	15.8 ± 0.2
KING	15.2 ± 0.2	17.5 ± 0.4	15.2 ± 0.2	17.1 ± 0.4	15.2 ± 0.1	17.7 ± 0.2	15.2 ± 0.1	17.2 ± 0.1
LEED	15.4 ± 0.3	16.8 ± 0.5	15.3 ± 0.2	16.3 ± 0.4	15.3 ± 0.1	16.9 ± 0.1	15.3 ± 0.1	16.4 ± 0.1
LOND	n/a	n/a	15.0 ± 0.3	18.2 ± 0.6	n/a	n/a	15.0 ± 0.3	18.3 ± 0.5
MALG	15.0 ± 0.6	13.5 ± 1.0	15.7 ± 0.3	14.5 ± 0.4	15.2 ± 0.3	14.4 ± 0.5	15.7 ± 0.1	14.1 ± 0.2
NEWC	15.2 ± 0.3	16.2 ± 0.5	15.2 ± 0.3	15.8 ± 0.4	15.2 ± 0.1	16.3 ± 0.2	15.1 ± 0.1	15.9 ± 0.2
OSHQ	n/a	n/a	15.1 ± 0.3	17.2 ± 0.4	n/a	n/a	15.1 ± 0.1	17.2 ± 0.2
THUR	15.8 ± 0.4	14.0 ± 0.7	15.6 ± 0.3	14.6 ± 0.4	15.7 ± 0.2	14.4 ± 0.3	15.7 ± 0.2	14.5 ± 0.2

standard deviations) between solutions DDRNF and PPPGTF to be 0.1 ± 0.4 and 0.4 ± 0.7 mm yr^{-1}, for north and east, respectively. Again, we find excellent overall agreement between the different solutions, that is, the CGPS processing strategies.

We further investigated the effect of spatial filtering on the horizontal velocities by computing the mean of the velocity differences (and their corresponding standard deviations) between solutions DDRNU and DDRNF to be -0.0 ± 0.1 and -0.3 ± 0.5 mm yr^{-1}, for north and east, respectively, and between solutions PPPGTU and PPPGTF to be 0.1 ± 0.3 and -0.0 ± 0.1 mm yr^{-1}, for north and east, respectively. We find excellent overall agreement between the velocity estimates of the unfiltered and filtered coordinate time-series. Therefore, we conclude that we have largely avoided de-coupling our horizontal station velocity estimates from their given reference frames.

Although we have shown excellent agreements between the four coordinate time-series solutions, with standard deviations in the velocity differences of less than 0.4 mm yr^{-1} for the north and less than 0.7 mm yr^{-1} for the east component, there are several stations for which the velocity differences are greater than 1.0 mm yr^{-1} in at least one comparison. We can list those stations to be CARD, IOMN, IOMS, MORP, NSTG, PMTG and SUNB. In almost all cases the large velocity differences are in the east component of the involved station. We associate the discrepancies for CARD with a shorter coordinate time-series of only 2.9 yr and a data gap in early 2005; for IOMN and IOMS with their east velocity estimate in solution DDRNU, which might be affected by data gaps during 2005; for MORP and NSTG with their general data quality issues (Teferle 2003); for PMTG potentially due to a shorter coordinate time-series and/or our modelling, and for SUNB with the significantly different data span used by both CGPS processing strategies, that is, solutions DDRNU and DDRNF were based on 8.7 yr whereas solutions PPPGTU and PPPGTF were based on only 6 yr. Considering these findings we will concentrate on solutions DDRNF and PPPGTF in our discussions of the horizontal crustal motions in Section 4.4.

4.1.2 Vertical station velocities

It is generally accepted that the vertical component of CGPS coordinate time-series is less well determined than the horizontal components, hence we do not expect the excellent agreements found in the north and east velocity estimates between the four solutions to be repeated in our vertical station velocity estimates. Additionally, the data time span will have a more significant effect on the estimates and as the coordinate time-series for solutions PPPGTU and PPPGTF are capped at 5 yr, this will affect the comparison between the two CGPS processing strategies. Furthermore, any other CGPS processing strategy-specific effects may be more pronounced in the vertical component and affect our station velocity estimates.

We obtained the vertical station velocity estimates and their associated uncertainties from the MLE for all four coordinate time-series solutions (Table 7 and Table S2 of the Supporting Information). The velocities range from -2.8 to 3.3, -2.0 to 1.5, -2.6 to 2.3 and -1.7 to 1.6 mm yr^{-1} for solutions DDRNU, PPPGTU, DDRNF and PPPGTF, respectively. This suggests not only that the spread is somewhat processing strategy dependent, but also that spatial filtering reduces the spread for both strategies. Similarly, we show the vertical station velocity uncertainties for solutions DDRNU, PPPGTU, DDRNF and PPPGTF to range from ±0.5 to ±2.4, ±0.7 to ±5.5, ±0.4 to ±1.9 and ±0.2 to ±5.1 mm yr^{-1}, respectively. Although these ranges appear to be quite large, it is shown that the upper bounds in all ranges are related to station CARD. We compute the mean of the velocity uncertainties (and their corresponding standard deviations) for solutions DDRNU, PPPGTU, DDRNF and PPPGTF to be 0.9 ± 0.4, 1.1 ± 0.8, 0.6 ± 0.3 and 0.7 ± 0.8 mm yr^{-1}, respectively. We point out that, first, solutions DDRNU and DDRNF seem to be more homogeneous than solutions PPPGTU and PPPGTF, as both the mean velocity uncertainties and their standard deviations are smaller, and, secondly, that spatial filtering clearly improved the homogeneity of solutions DDRNF and PPPGTF by reducing the mean velocity uncertainties.

Considering the mean of the vertical station velocity differences (and their corresponding standard deviations) between solutions DDRNU and DDRNF, and solutions PPPGTU and PPPGTF, we compute these to be 0.2 ± 0.6 and -0.1 ± 0.5 mm yr^{-1}, respectively, confirming that the effect of spatial filtering on the vertical station velocity estimates is negligible, and that we have again avoided a de-coupling from the given reference frame. However, when considering the mean of the velocity differences (and their corresponding standard deviations) between solutions DDRNU and PPPGTU and solutions DDRNF and PPPGTF, we compute these to be 1.1 ± 1.1 and 0.7 ± 0.6 mm yr^{-1}, respectively, which suggests a systematic bias in the vertical station velocity estimates between the regional and global solutions for both the unfiltered and filtered cases. Similar biases between different solutions and/or their reference frame implementations have previously been reported on (e.g. Mazzotti *et al.* 2008; Teferle *et al.* 2008).

Considering the vertical station velocity estimates and their uncertainties in Table 7 on a station-by-station basis, then we can say that for CARD, HEMS, HERT and RAL1, and potentially also for BLAK, IOMN, IOMS and MALG the velocity estimates are affected by the shorter data time span. Besides this, there have been issues with data quality for ABER, MORP and NSTG (Teferle 2003; Teferle *et al.* 2003). In addition to the stations already mentioned, there are two CGPS stations which exhibit velocity differences of greater than 1 mm yr^{-1} between one of their unfiltered and filtered solutions, these are LIVE and NPLD.

Table 7. CGPS vertical station velocity estimates for unfiltered GAS2.4 DD regional network (DDRNU), unfiltered BSW5.0 globally transformed PPP (PPPGTU), filtered GAS2.4 DD regional network (DDRNF) and filtered BSW5.0 globally transformed PPP (PPPGTF) coordinate time-series solutions. All values are in mm yr^{-1}. Uncertainties are 1σ.

	DDRNU (mm yr^{-1})	PPPGTU (mm yr^{-1})	DDRNF (mm yr^{-1})	PPPGTF (mm yr^{-1})
		CGPS@TG stations		
ABER	1.6 ± 0.7	-0.9 ± 1.0	1.3 ± 0.3	-0.3 ± 0.4
BRST	1.5 ± 0.8	n/a	1.3 ± 0.6	n/a
LIVE	0.1 ± 0.9	0.8 ± 1.1	1.1 ± 0.3	1.1 ± 0.4
LOWE	0.0 ± 0.6	-0.6 ± 0.7	0.0 ± 0.5	-0.6 ± 0.3
NEWL	1.1 ± 1.1	0.1 ± 0.8	0.6 ± 0.9	0.1 ± 0.7
NSTG	0.5 ± 1.0	0.1 ± 1.1	0.1 ± 0.8	0.3 ± 0.5
PMTG	0.7 ± 1.0	-0.6 ± 0.9	0.5 ± 0.7	-0.6 ± 0.4
SHEE	0.4 ± 0.6	-0.2 ± 0.9	0.5 ± 0.5	-0.2 ± 0.6
		Other scientific CGPS stations		
ABYW	0.6 ± 0.9	-0.5 ± 0.8	0.9 ± 0.6	-0.7 ± 0.4
BARK	-0.2 ± 0.5	-0.6 ± 0.9	-0.1 ± 0.5	-0.6 ± 0.5
CAMB	0.8 ± 0.8	-1.5 ± 0.9	0.5 ± 0.4	-0.8 ± 0.6
CARD	2.2 ± 2.4	-1.4 ± 5.5	0.1 ± 1.9	-1.5 ± 5.1
DUNK	0.5 ± 0.6	-0.2 ± 1.5	0.2 ± 0.4	-0.8 ± 1.1
HEMS	0.4 ± 1.5	n/a	1.7 ± 1.2	n/a
HERS	-0.4 ± 0.9	0.4 ± 1.0	-0.3 ± 0.8	0.1 ± 0.6
HERT	n/a	1.4 ± 1.8	n/a	0.4 ± 1.1
HURN	0.7 ± 0.8	-0.2 ± 0.9	0.3 ± 0.5	-0.1 ± 0.4
IESG	-0.9 ± 0.6	-0.6 ± 0.7	-0.8 ± 0.3	-0.6 ± 0.2
LERW	0.9 ± 0.8	-0.1 ± 0.7	0.8 ± 0.5	-0.1 ± 0.5
MORP	0.6 ± 1.4	-2.0 ± 2.5	0.3 ± 1.1	-1.7 ± 2.0
NPLD	0.9 ± 0.7	-1.8 ± 1.0	0.1 ± 0.5	-0.3 ± 0.4
PERS	0.2 ± 0.7	-1.3 ± 1.0	0.0 ± 0.4	-0.5 ± 0.3
RAL1	-2.8 ± 1.6	n/a	-2.6 ± 1.1	n/a
SUNB	-0.9 ± 0.7	-1.0 ± 0.9	-0.8 ± 0.6	-1.2 ± 0.6
		Network RTK CGPS stations		
BLAK	n/a	0.9 ± 1.2	n/a	0.5 ± 0.4
CARL	1.8 ± 0.8	0.3 ± 0.8	1.2 ± 0.4	0.7 ± 0.3
COLC	n/a	-0.7 ± 0.8	n/a	-0.1 ± 0.3
DARE	1.5 ± 0.7	0.0 ± 0.8	1.0 ± 0.5	0.5 ± 0.3
EDIN	2.3 ± 0.8	1.5 ± 0.7	2.2 ± 0.5	1.6 ± 0.3
GLAS	2.5 ± 0.7	1.0 ± 0.8	2.3 ± 0.4	1.0 ± 0.3
INVE	0.9 ± 0.8	0.1 ± 0.8	1.0 ± 0.5	0.1 ± 0.5
IOMN	2.2 ± 1.3	0.8 ± 1.2	1.7 ± 0.9	1.2 ± 0.8
IOMS	1.5 ± 1.0	0.0 ± 0.8	0.9 ± 0.6	0.4 ± 0.3
KING	-0.3 ± 0.6	-0.3 ± 0.7	-0.3 ± 0.4	-0.5 ± 0.2
LEED	-0.3 ± 0.5	0.0 ± 0.7	0.0 ± 0.3	-0.3 ± 0.2
LOND	n/a	-0.9 ± 1.4	n/a	-0.4 ± 1.1
MALG	3.2 ± 1.8	0.7 ± 0.8	2.2 ± 1.0	0.9 ± 0.4
NEWC	0.5 ± 0.7	1.4 ± 1.0	0.8 ± 0.4	0.9 ± 0.6
OSHQ	n/a	-0.1 ± 0.7	n/a	-0.3 ± 0.4
THUR	2.2 ± 0.9	0.2 ± 0.9	1.7 ± 0.4	0.4 ± 0.5

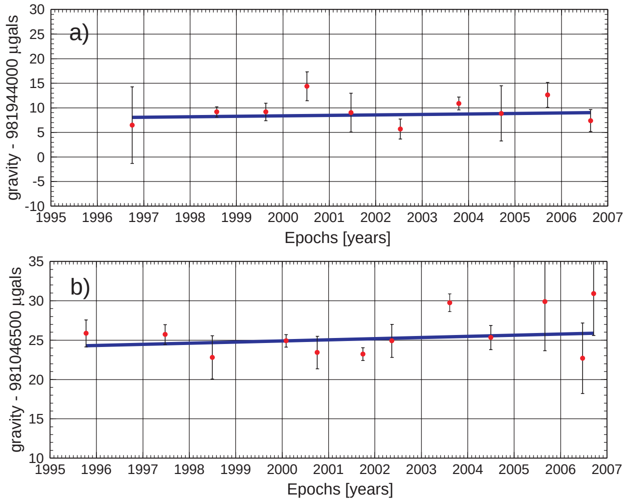

Figure 4. Absolute gravity time-series for Lerwick (a), and Newlyn (b) AG stations used in this study. The red dots show the AG estimates of absolute gravity and the blue line represents the best-fitting linear trend in the absolute gravity estimates.

Based on the results presented in this section, we conclude that parallel processing with two or more independent CGPS processing strategies is essential in order to make the best use of stations that have data of varying quality. We note that when considered together with the vertical crustal motion estimates from the geological information (below), it is suggested that the more realistic solutions for ABER, DUNK and NPLD might be DDRNU and DDRNF whereas the more realistic solutions for MALG, NSTG and LIVE might be PPPGTU and PPPGTF.

4.2 Absolute gravity

The AG time-series for Newlyn and Aberdeen are shown in Fig. 4. A visual inspection shows that there appears to be a positive change in AG at both Lerwick and Newlyn AG stations, which would equate to subsidence at those sites. We do not show the time-series for the AG station in Aberdeen in Fig. 4 as we see a very bimodal distribution in the results. This could be a result of local hydrological conditions at the site. The church in which the AG measurements are made, is at the edge of the granitic bedrock in Aberdeen on a sliver of conglomerate and situated next to alluvial sediments in the valley of the river Don. We assume that due to local hydrological conditions, our current AG results for this station are not reliable and would need to be treated with extreme caution. In the future, we may need to locate a new AG site in Aberdeen or perhaps measure in winter when the soil may become completely saturated giving a more constant gravity effect (Lambert *et al.* 2006). Therefore, we did not include the estimated changes in AG or vertical station velocity for the AG station in Aberdeen in our further analysis.

As stated in above, we have not attempted to correct for any hydrological variations. At Newlyn and Lerwick we are confident that the hydrological conditions produce only minimal annual variations that are further limited by the fact that we measure annually at nearly the same time each year. The church at Newlyn is built on solid granite bedrock with minimal soil cover and the basement of the school in Lerwick is surrounded by a concrete cap, which should minimize rainfall infiltration into the soil in the nearby vicinity. However, we do intend to study the hydrological conditions at all three sites in the future. For Lerwick and Newlyn, we estimate changes in AG and their uncertainties of $+0.10 \pm 0.19$ and $+0.14 \pm 0.14\,\mu\text{Gal yr}^{-1}$, and of vertical station velocities and their uncertainties of -0.5 ± 1.0 and $-0.7 \pm 0.7\,\text{mm yr}^{-1}$, respectively. The increased noise in the last few Newlyn campaigns reflects an increase in day-to-day scatter of those data sets. This can be partly explained by a noticeable increase in the scatter of the superspring in FG5-103 over the last few years. However, since no comparable increase is evident in the results at Lerwick another, so far unexplained, factor must also be involved that is perhaps local to Newlyn.

At this stage, we point to Appendix B which discusses the levelling ties between the AG station and the TG benchmarks at Newlyn, and serves to validate the AG-alignment procedure carried out later.

4.3 Geological information

Shennan & Horton (2002) and Shennan *et al.* (2006) obtained estimates of vertical crustal motions based on Holocene sea level data for over 50 locations in Great Britain to form a map. For completeness we list a subset of these sites, which are of interest for this study owing to their proximity to the CGPS and AG stations, in Table 4 together with their estimates of vertical crustal motion.

4.4 Horizontal crustal motions

We obtain estimates of horizontal crustal motions for Great Britain from our horizontal CGPS station velocity estimates if we assume that the apparent station displacement is solely due to motion of the Earth's crust and does not include any movement associated with the location or monumentation of the CGPS station. In this case Figs 5(a) and (b) show the absolute horizontal station velocity estimates for solutions DDRNF and PPPGTF, respectively. Also shown are velocities computed for the CGPS stations in Great Britain based on the ITRF2000 plate motion model (Altamimi *et al.* 2002, Table S3 of the Supporting Information).

From Figs 5(a) and (b), we can see that there is generally good agreement in both direction and magnitude of the velocity vectors between both solutions and the model. However, a better impression of the agreement at a particular CGPS station is gained by looking at the residual velocities, i.e. after subtracting the ITRF2000 plate motion model velocities (Altamimi *et al.* 2002). The residual velocities will show to what extent the CGPS stations move according to the plate motion model, but also, more importantly at this stage, will show which stations do not behave in an expected manner. As mentioned previously, we expect a horizontal GIA signal at the 1-2 mm yr^{-1} level (Bradley *et al.* 2009) to be superimposed onto the observed plate motion. In addition, since only a few CGPS stations in Great Britain are believed to have appropriate geodetic-quality monumentation, we cannot ignore the possibility of additional movements due to local factors.

Since we do not estimate integer ambiguities in either solution, we would expect the east component velocities to be somewhat biased (e.g. Johansson *et al.* 2002). Therefore, we do not investigate the plate motion signal in Great Britain any further at this stage, but instead try to identify those stations that seem to behave in a consistent manner, ensuring their use in our investigations into the horizontal component of the GIA signal.

Figs 5(c) and (d) show the residual velocity vectors for solutions DDRNF and PPPGTF given in Table 8. Comparing the horizontal velocity vectors from both solutions, there are a number of stations, which show excellent agreement with the ITRF2000 plate motion

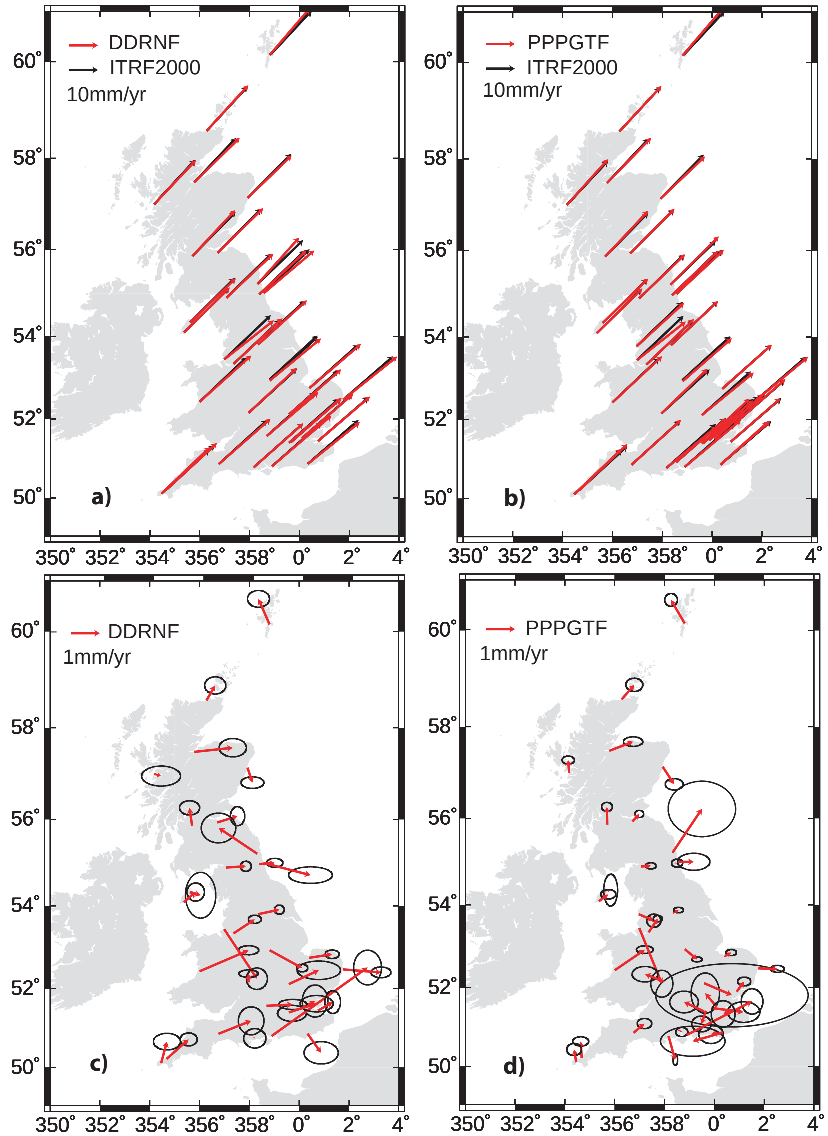

Figure 5. Absolute and residual horizontal station velocities for filtered GAS2.4 DD regional network (DDRNF) and BSW5.0 globally transformed PPP (PPPGTF) time-series solutions. Computed horizontal station velocities are compared to the ITRF2000 plate motion model velocities and residual velocities have been computed by subtracting the ITRF2000 plate motion model velocities from the computed velocities. Note the change in scale for the residual velocities. Error ellipses are at the 95 per cent confidence level and their scale is that of the residual velocities.

model. There are obviously also stations with fewer similarities to the plate motion model in their residuals and some showing much larger residuals. Stations with residuals visibly larger than 1 mm yr^{-1} in both solutions are ABYW, LIVE, MORP and PMTG, while NSTG shows a large residual only for solution DDRNF. However, it is important to note that we have already identified these CGPS stations as likely to give unreliable results based on their data quality.

From Figs 5(c) and (d) as well as Table 8 it is noticeable that for a number of stations there are large differences in their error ellipses and uncertainties, respectively. Primarily, these depend on the length of the coordinate time-series and magnitude of their day-to-day scatter, which is a reflection of the amount of noise and the ratio of its white and coloured noise components. Ultimately, the uncertainties will also depend on how well a particular coordinate time-series can be modelled, as velocity, offsets, periodic signals, and noise, and on how much spatial filtering improves the time-series and subsequently the final model fit. A more detailed investigation of the stochastic properties of the coordinate time-series on station-specific and solution-specific effects would go beyond the scope of this study.

From a geophysical perspective, the estimates of absolute and residual horizontal crustal motion confirm that overall Great Britain behaves in a consistent manner with Eurasia plate motion and that there is, with the current resolution, no discernible internal deformation in the horizontal velocity field over the area investigated. Contrary to previous studies (Nocquet *et al.* 2001; Nocquet & Calais 2003), our results do not confirm any residual motion of southeast England with respect to Eurasia.

Further investigation reveals a distribution depending on two categories of monumentation used. We can separate stations believed to be sufficiently connected to bedrock (either via a carbon-fibre pole with stainless steel ends attached to a submerged concrete block that rests directly on top of bedrock, or via a large structure, i.e. Barking Barrier) from those mounted on roofs or walls of single to

Table 8. Residual horizontal station velocity estimates computed for the filtered GAS2.4 DD regional network (DDRNF) and filtered BSW5.0 globally transformed PPP (PPPGTF) coordinate time-series solutions by subtracting ITRF2000 plate motion model estimates for each CGPS station. All values are in mm yr^{-1}. Uncertainties are 1σ.

	DDRNF			PPPGTF		
	North (mm yr^{-1})	East (mm yr^{-1})	horiz. (mm yr^{-1})	North (mm yr^{-1})	East (mm yr^{-1})	horiz. (mm yr^{-1})
			CGPS@TG stations			
ABER	-0.5 ± 0.2	0.2 ± 0.3	0.5	-0.6 ± 0.2	0.4 ± 0.3	0.7
LIVE	-1.7 ± 0.3	1.1 ± 0.3	2.1	-1.9 ± 0.4	0.8 ± 0.3	2.1
LOWE	-0.1 ± 0.2	1.3 ± 0.3	1.3	0.0 ± 0.1	0.7 ± 0.2	0.7
NEWL	0.8 ± 0.2	0.2 ± 0.4	0.8	0.4 ± 0.2	-0.1 ± 0.2	0.5
NSTG	-0.4 ± 0.2	1.6 ± 0.6	1.7	0.0 ± 0.2	0.5 ± 0.5	0.5
PMTG	2.4 ± 0.5	3.3 ± 0.4	4.1	1.2 ± 0.4	2.3 ± 0.3	2.5
SHEE	0.3 ± 0.3	0.5 ± 0.2	0.6	-0.2 ± 0.4	-0.3 ± 0.3	0.4
			Other scientific CGPS stations			
ABYW	0.7 ± 0.1	1.7 ± 0.3	1.8	0.7 ± 0.1	1.0 ± 0.2	1.3
BARK	0.2 ± 0.5	0.5 ± 0.4	0.5	0.5 ± 0.6	-0.4 ± 0.4	0.6
CAMB	0.7 ± 0.2	0.8 ± 0.2	1.0	0.6 ± 0.1	0.0 ± 0.2	0.6
CARD	0.5 ± 0.3	1.0 ± 0.6	1.1	-0.4 ± 0.9	1.0 ± 2.1	1.1
DUNK	0.4 ± 0.4	1.1 ± 0.4	1.2	0.3 ± 0.1	0.4 ± 0.2	0.5
HERS	-0.7 ± 0.3	0.5 ± 0.5	0.8	-0.1 ± 0.3	-0.4 ± 0.3	0.4
HERT	n/a	n/a		-0.3 ± 0.4	-1.0 ± 0.9	1.1
HURN	0.0 ± 0.3	0.0 ± 0.3	0.1	-0.8 ± 0.2	0.2 ± 0.1	0.9
IESG	-0.6 ± 0.1	1.1 ± 0.2	1.3	-0.4 ± 0.1	0.4 ± 0.1	0.6
LERW	0.9 ± 0.2	-0.4 ± 0.3	1.0	0.8 ± 0.2	-0.5 ± 0.2	0.9
MORP	0.9 ± 0.4	-1.3 ± 0.5	1.6	1.5 ± 0.8	1.0 ± 0.9	1.8
NPLD	-0.1 ± 0.2	0.0 ± 0.4	0.1	-0.5 ± 0.2	-0.2 ± 0.3	0.5
PERS	0.3 ± 0.1	0.0 ± 0.3	0.3	0.2 ± 0.2	-0.6 ± 0.4	0.7
RAL1	0.0 ± 0.1	0.9 ± 0.4	0.9	n/a	n/a	
SUNB	0.3 ± 0.2	1.0 ± 0.5	1.0	0.3 ± 0.3	-0.7 ± 0.4	0.8
			Network RTK CGPS stations			
BLAK	n/a	n/a		-0.2 ± 0.2	0.5 ± 0.2	0.6
CARL	0.0 ± 0.1	0.7 ± 0.2	0.7	0.0 ± 0.1	0.3 ± 0.1	0.3
COLC	n/a	n/a		0.4 ± 0.1	0.3 ± 0.2	0.4
DARE	0.5 ± 0.1	0.7 ± 0.2	0.9	0.5 ± 0.1	0.3 ± 0.1	0.6
EDIN	0.2 ± 0.3	0.7 ± 0.2	0.7	0.3 ± 0.1	0.2 ± 0.1	0.4
GLAS	0.6 ± 0.2	-0.1 ± 0.3	0.6	0.6 ± 0.1	0.0 ± 0.2	0.6
INVE	0.1 ± 0.3	1.3 ± 0.4	1.3	0.3 ± 0.1	0.8 ± 0.3	0.9
IOMN	-0.1 ± 0.6	0.4 ± 0.4	0.4	0.0 ± 0.4	0.2 ± 0.2	0.2
IOMS	0.4 ± 0.3	0.4 ± 0.2	0.5	0.2 ± 0.1	0.3 ± 0.2	0.4
KING	0.1 ± 0.1	0.8 ± 0.2	0.8	0.1 ± 0.1	0.2 ± 0.1	0.3
LEED	0.2 ± 0.1	0.7 ± 0.1	0.8	0.1 ± 0.1	0.2 ± 0.1	0.2
LOND	n/a	n/a		-0.1 ± 0.3	1.1 ± 0.5	1.1
MALG	-0.1 ± 0.3	0.2 ± 0.5	0.3	0.4 ± 0.1	0.0 ± 0.2	0.4
NEWC	0.0 ± 0.1	0.5 ± 0.2	0.5	0.0 ± 0.1	0.1 ± 0.2	0.1
OSHQ	n/a	n/a		-0.1 ± 0.1	0.1 ± 0.2	0.1
THUR	0.5 ± 0.2	0.3 ± 0.3	0.6	0.5 ± 0.2	0.4 ± 0.2	0.7

multistorey brick buildings (Table 2, Figs 6a and b). As some of the time-series are still just above the minimum recommended length of 2.5 yr we show the residual horizontal station velocities against the time span used for both categories of monumentation (Figs 6c and d). Unfortunately, our results presented in Fig. 6 are inconclusive. There may be a suggestion that stations on brick buildings give similar results to those of bedrock stations, independent of solutions, as there is no clear separation. Also, the time span does not seem to have a large effect on the residual velocity magnitude. This is not necessarily what we would have expected, but it confirms some of the findings of Calais *et al.* (2006) and, in a way also, of Beavan (2005).

Overall, ignoring the five stations with very large residuals, the magnitude of the residuals is larger for those of solution DDRNF than for PPPGTF. We can confirm this by comparing Figs 6(a) and (b), and by computing the root-mean-square (rms) statistic of the residuals, which is 1.0 and 0.7 mm yr^{-1} for solutions DDRNF and PPPGTF, respectively.

From Table 8 we can also compute that for solution DDRNF the RMS of the north component residuals is less than for the east component residuals, confirming either the aforementioned possible bias in our east component due to not fixing ambiguities to integers or a symptom of the reference frame implementation for this solution. However, as the east component residuals of solution PPPGTF are just slightly larger than the north component residuals, this might be an indication that the source of the bias in solution DDRNF is largely due to the particular reference frame implementation and only to a small degree due to the float ambiguities.

Nevertheless, we have shown that overall our horizontal station velocity estimates do not appear to be affected by monumentation

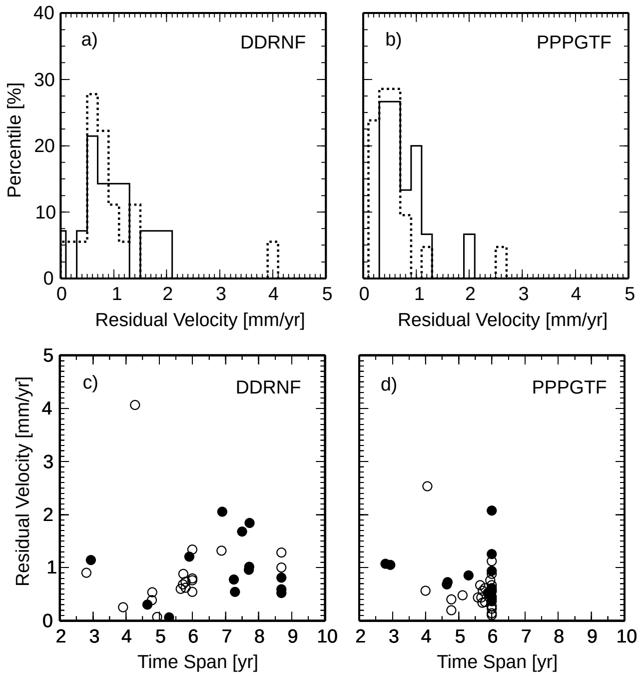

Figure 6. Residual horizontal station velocities distribution and residual horizontal station velocities versus time span for filtered GAS2.4 DD regional network (DDRNF) and filtered BSW5.0 globally transformed PPP (PPPGTF) coordinate time-series solutions. Solid lines in (a) and (b) and solid circles in (c) and (d) represent CGPS stations believed to be connected to bedrock either directly (carbon-fibre pole on concrete block) or via a large structure. The dotted lines and open circles represent CGPS stations mounted on roofs or walls of single to multistorey brick buildings.

or time span. Although, we cannot rule out local movements, which might explain some of the residual velocities, we have identified a list of stations that have the potential to be useful for further investigations into the horizontal crustal motion components of the GIA signal in Great Britain.

4.5 Vertical crustal motions

We obtain estimates of vertical crustal motions for Great Britain from our vertical station velocity estimates if we assume that the apparent station displacement is solely due to motion of the Earth's crust and does not include any local movement associated with the location or monumentation of the CGPS station. In order to achieve this, we compare the CGPS and AG estimates of vertical station velocities with each other, compute AG-aligned CGPS estimates (Teferle *et al.* 2006) and compare the AG-aligned CGPS estimates with the independent evidence of vertical crustal motions from the Holocene sea level data for Great Britain.

Several authors have published alternative and independent evidence for vertical crustal motions in Great Britain which include estimates based on geological information, sea level observations and predictions from GIA models. As reported by Teferle *et al.* (2006), it is possible to carry out comparisons of the geodetic estimates of vertical crustal motions from AG and CGPS to those alternative data sets.

Teferle *et al.* (2006) compared their vertical station velocity estimates from CGPS and AG at Newlyn and Lerwick and found that the CGPS velocities were on average $1.0 \pm 0.8\,\mathrm{mm\,yr^{-1}}$ more positive than those from AG. When they applied this correction to

Table 9. Comparison of AG and CGPS estimates of vertical station velocities for the unfiltered GAS2.4 DD regional network (DDRNU), the unfiltered BSW5.0 globally transformed PPP (PPPGTU), the filtered GAS2.4 DD regional network (DDRNF), and the filtered BSW5.0 globally transformed PPP (PPPGTF) coordinate time-series solutions.

Station name	Station ID	CGPS minus AG difference			
		DDRNU ($\mathrm{mm\,yr^{-1}}$)	PPPGTU ($\mathrm{mm\,yr^{-1}}$)	DDRNF ($\mathrm{mm\,yr^{-1}}$)	PPPGTF ($\mathrm{mm\,yr^{-1}}$)
Lerwick	LERW	+1.4	+0.4	+1.3	+0.4
Newlyn TG	NEWL	+1.8	+0.9	+1.4	+0.9
Weighted mean		+1.5	+0.6	+1.3	+0.6
Standard deviation		±0.3	±0.3	±0.1	±0.3

Table 10. AG-aligned CGPS vertical station velocity estimates for the unfiltered GAS2.4 DD regional network (DDRNU), the unfiltered BSW5.0 globally transformed PPP (PPPGTU), the filtered GAS2.4 DD regional network (DDRNF), and the filtered BSW5.0 globally transformed PPP (PPPGTF) coordinate time-series solutions. All uncertainties are 1σ.

Station ID	DDRNU ($\mathrm{mm\,yr^{-1}}$)	PPPGTU ($\mathrm{mm\,yr^{-1}}$)	DDRNF ($\mathrm{mm\,yr^{-1}}$)	PPPGTF ($\mathrm{mm\,yr^{-1}}$)
		CGPS@TG stations		
ABER	0.1 ± 0.7	−1.5 ± 1.0	0.0 ± 0.3	−0.8 ± 0.5
BRST	0.0 ± 0.8	n/a	0.0 ± 0.6	n/a
LIVE	−1.5 ± 0.9	0.2 ± 1.1	−0.2 ± 0.3	0.5 ± 0.4
LOWE	−1.5 ± 0.6	−1.2 ± 0.7	−1.3 ± 0.5	−1.2 ± 0.4
NEWL	−0.5 ± 1.1	−0.5 ± 0.9	−0.7 ± 0.9	−0.4 ± 0.7
NSTG	−1.0 ± 1.0	−0.5 ± 1.1	−1.2 ± 0.8	−0.3 ± 0.5
PMTG	−0.9 ± 1.0	−1.2 ± 1.0	−0.8 ± 0.7	−1.1 ± 0.5
SHEE	−1.1 ± 0.6	−0.8 ± 1.0	−0.7 ± 0.5	−0.8 ± 0.7
		Other scientific CGPS stations		
ABYW	−0.9 ± 0.9	−1.1 ± 0.8	−0.4 ± 0.6	−1.2 ± 0.5
BARK	−1.7 ± 0.6	−1.2 ± 0.9	−1.4 ± 0.5	−1.2 ± 0.5
CAMB	−0.7 ± 0.8	−2.1 ± 0.9	−0.7 ± 0.4	−1.3 ± 0.6
CARD	0.7 ± 2.4	−2.0 ± 5.5	−1.2 ± 1.9	−2.1 ± 5.1
DUNK	−1.0 ± 0.7	−0.7 ± 1.5	−1.1 ± 0.4	−1.4 ± 1.1
HERS	−1.9 ± 0.9	−0.2 ± 1.0	−1.6 ± 0.8	−0.4 ± 0.7
HERT	n/a	0.8 ± 1.8	n/a	−0.2 ± 1.1
HURN	−0.9 ± 0.9	−0.8 ± 0.9	−1.0 ± 0.5	−0.7 ± 0.5
IESG	−2.4 ± 0.6	−1.2 ± 0.7	−2.1 ± 0.3	−1.1 ± 0.3
LERW	−0.6 ± 0.8	−0.7 ± 0.7	−0.5 ± 0.5	−0.6 ± 0.5
NPLD	−0.6 ± 0.7	−2.4 ± 1.0	−1.1 ± 0.5	−0.9 ± 0.5
PERS	−1.3 ± 0.8	−1.9 ± 1.0	−1.3 ± 0.4	−1.1 ± 0.4
SUNB	−2.4 ± 0.7	−1.6 ± 0.9	−2.1 ± 0.6	−1.7 ± 0.7
		Network RTK CGPS stations		
BLAK	n/a	0.3 ± 1.3	n/a	−0.1 ± 0.4
CARL	0.3 ± 0.8	−0.3 ± 0.9	−0.1 ± 0.4	0.1 ± 0.4
COLC	n/a	−1.2 ± 0.8	n/a	−0.6 ± 0.4
DARE	0.0 ± 0.7	−0.6 ± 0.8	−0.3 ± 0.5	−0.1 ± 0.4
EDIN	0.8 ± 0.8	0.9 ± 0.8	0.9 ± 0.5	1.1 ± 0.3
GLAS	1.0 ± 0.7	0.5 ± 0.8	1.0 ± 0.4	0.5 ± 0.4
INVE	−0.6 ± 0.9	−0.5 ± 0.9	−0.2 ± 0.5	−0.4 ± 0.6
IOMN	0.7 ± 1.3	0.2 ± 1.2	0.4 ± 1.0	0.6 ± 0.9
IOMS	−0.1 ± 1.0	−0.6 ± 0.8	−0.4 ± 0.6	−0.1 ± 0.4
KING	−1.9 ± 0.6	−0.9 ± 0.7	−1.5 ± 0.4	−1.1 ± 0.3
LEED	−1.8 ± 0.6	−0.6 ± 0.8	−1.3 ± 0.3	−0.8 ± 0.3
LOND	n/a	−1.5 ± 1.5	n/a	−0.9 ± 1.1
MALG	1.7 ± 1.8	0.1 ± 0.8	0.9 ± 1.0	0.4 ± 0.4
MORP	−0.9 ± 1.4	−2.6 ± 2.5	−1.0 ± 1.1	−2.3 ± 2.0
NEWC	−1.0 ± 0.7	0.8 ± 1.0	−0.5 ± 0.4	0.4 ± 0.6
THUR	0.7 ± 0.9	−0.4 ± 0.9	0.4 ± 0.4	−0.1 ± 0.6

the CGPS velocities the agreement between their CGPS estimates of vertical crustal motions and those from geology, sea level and the GIA models improved significantly.

Using our vertical station velocities from AG and CGPS, a comparison between the CGPS and AG vertical station velocities can be made for stations close to Lerwick TG on Shetland and close to or at the Newlyn TG in southwest England. We show the results of this comparison in Table 9.

As stated previously, the mean offset (and its corresponding standard deviation) between the CGPS estimates of vertical station velocity from the two software/processing strategies were 1.1 ± 1.1 mm yr^{-1} between solutions DDRNU and PPPGTU, and 0.7 ± 0.6 mm yr^{-1} between solutions DDRNF and PPPGTF, with the estimates of vertical station velocity based on DDRN being more positive than the estimates based on PPPGT. When considering AG, the weighted mean offset (and its corresponding standard deviation) suggest that all four of the CGPS estimates of vertical station velocity are systematically offset from the estimates based on AG: those from solutions DDRNU and DDRNF being more positive by 1.5 or 1.3 mm yr^{-1} and those from solutions PPPGTU and PPPGTF both being more positive by 0.6 mm yr^{-1}.

As Teferle *et al.* (2006) reported previously, several authors have also identified systematic offsets when comparing CGPS estimates of vertical station velocity to independent evidence; Prawirodirdjo & Bock (2004) compared CGPS estimates of vertical station velocity with estimates from a GIA model and reported an offset of +1.1 mm yr^{-1} for stations in North America and +1.7 mm yr^{-1} for stations in northern Europe, with the CGPS estimates being more positive than the GIA model, MacMillan (2004) compared CGPS and Very Long Baseline Interferometry (VLBI) and found that CGPS estimates of vertical station velocity were 1.5 mm yr^{-1} more positive than VLBI estimates at 22 co-located global stations,

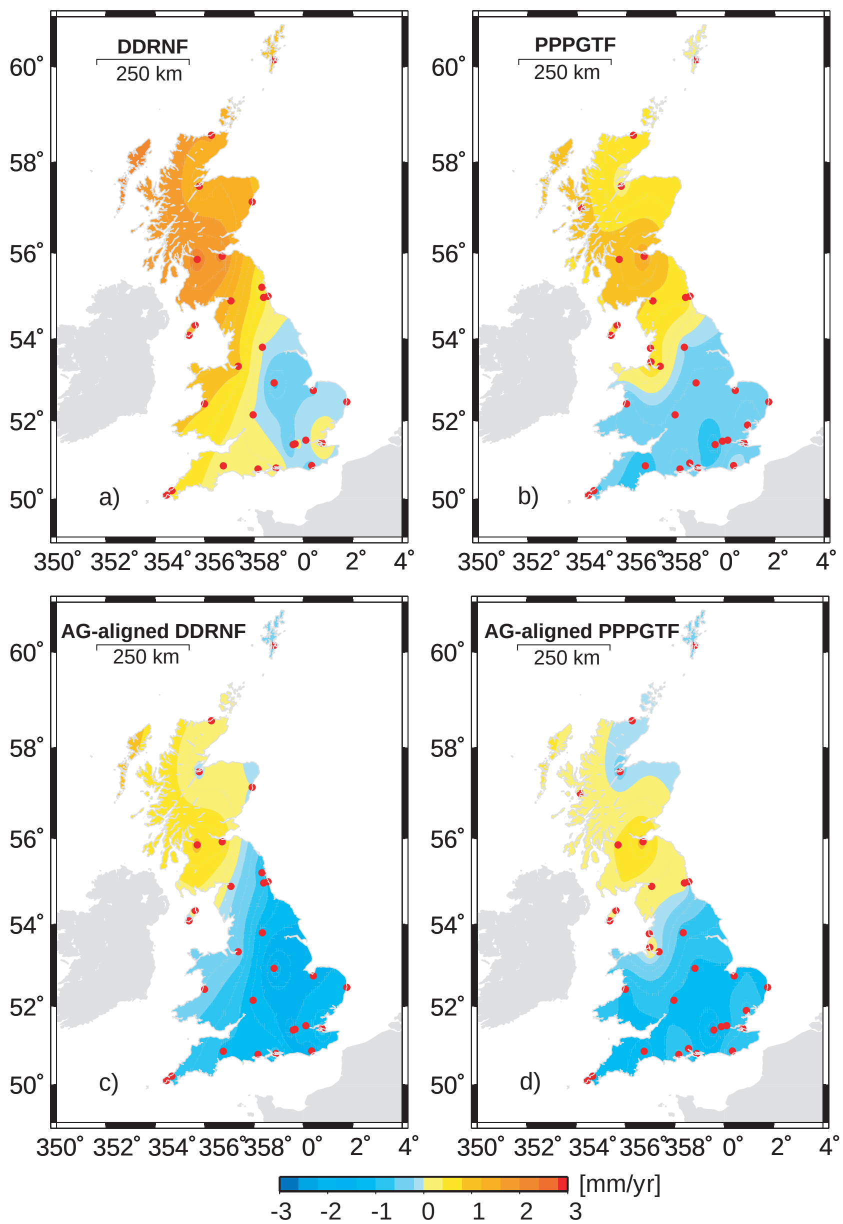

Figure 7. Maps of vertical crustal motions from CGPS estimates and AG-aligned CGPS estimates of vertical station velocity for filtered GAS2.4 DD regional network (DDRNF) and filtered BSW5.0 globally transformed PPP (PPPGTF) coordinate time-series solutions.

and finally, most recently, another study (Mazzotti *et al.* 2007) found their CGPS estimates of vertical station velocity to be more positive than those from AG by on average 2.2 ± 1.3 mm yr^{-1} for the northern Cascadia in the United States and Canada.

Presently, the general consensus in the international community is that current CGPS estimates of vertical station velocity may be systematically biased, which is due to a combination of: the use of models for relative antenna phase centre variations, that is, inadequate modelling of satellite and receiver antenna phase centres in a changing satellite constellation (e.g. Ge *et al.* 2005; Cardellach *et al.* 2007); the use of current terrestrial reference frames, such as ITRF2000 and ITRF2005 (e.g. Blewitt *et al.* 2006); and, in the case of solutions DDRNU and DDRNF, limitations in using a regional rather than a global network and reference frame implementation, for which we have already shown a systematic offset of +1.1 or +0.7 mm yr^{-1} when compared to solutions PPPGTU and PPPGTF, respectively.

With this in mind, we now assume that the presented vertical station velocity estimates for solutions PPPGTU and PPPGTF are truly with respect to ITRF2000. We have shown that in both cases these are systematically offset, that is, more positive, when compared to those from AG. The update to ITRF2005, the most recent terrestrial frame realization, however, brought about an increase of this systematic bias in our CGPS velocity estimates for both solutions. Altamimi *et al.* (2007) pointed out that due to a rate in the Z-translation of the ITRF2005 with respect to ITRF2000, the vertical component of ITRF2005 will differ by $+1.8 \times \sin(\phi)$ mm yr^{-1} to that of ITRF2000, with ϕ being the station latitude. At the same time, the ITRF2000 scale rate was shown to be 0.08 ppb yr^{-1} with respect to ITRF2005, which would reduce the contribution of the Z-translation rate to the vertical station velocity differences by 0.5 mm yr^{-1}. This means that for Great Britain, which lies between the latitudes of 50°N and 60°N, the ITRF2005 vertical station velocities will be about 0.9–1.1 mm yr^{-1}, respectively, larger than those of ITRF2000. However, with the current concerns about the correctness of the Z-translation rate (Altamimi *et al.* 2007; Argus 2007) and the other aforementioned issues related to antenna phase centre and atmospheric modelling, we decided to present our results based on ITRF2000. Interestingly, if we assume that the ITRF2000 scale rate, as determined with respect to ITRF2005, is correct, then the associated change in the vertical station velocities of 0.5 mm yr^{-1} would agree favourably with our systematic bias of 0.6 mm yr^{-1} between the CGPS and AG estimates of vertical station velocity for solutions PPPGTU and PPPGTF.

Teferle *et al.* (2006) presented a very simple procedure for combining CGPS and AG estimates of vertical station velocity, based on aligning the CGPS estimates to the AG estimates using the systematic offset between them. Following this procedure, we compute AG-aligned CGPS estimates of vertical station velocity, the systematic offset relating to a particular CGPS solution being basically subtracted from the CGPS estimate of vertical station velocity for a station. Through this procedure, the CGPS estimates of vertical station velocity presented in Table 7 are changed to the AG-aligned CGPS estimates given in Table 10, which only shows the reliable estimates (based on the discussions above).

It is clear from Table 10 that the AG-aligned CGPS estimates of vertical station velocity from solutions DDRNU, DDRNF, PPPGTU and PPPGTF are in much better agreement than the corresponding CGPS estimates of vertical station velocity. We show that the mean offset (and its corresponding standard deviation) between the estimates of vertical station velocity from the two CGPS software/processing strategies are reduced from $+1.1 \pm 1.1$ to $+0.1 \pm 1.1$ mm yr^{-1} between solutions DDRNU and PPPGTU, and from $+0.7 \pm 0.6$ to $+0.0 \pm 0.6$ mm yr^{-1} between solutions DDRNF and PPPGTF, when aligning the CGPS to the AG results. Appendix C includes further evidence for the validation of the AG-alignment procedure carried out, through comparison of the CGPS and AG-aligned CGPS estimates of vertical station velocity for ABER, BRST and NEWL with results from Wöppelmann *et al.* (2007), a recent analysis as part of the IGS TIGA Pilot-Project.

The effect of the AG-alignment procedure on the vertical crustal motions for Great Britain can be clearly seen in Fig. 7. This figure shows maps of vertical crustal motions from CGPS estimates and AG-aligned CGPS estimates of vertical station velocity for solutions DDRNF and PPPGTF.

For comparison we also show a map of vertical crustal motions for Great Britain derived from the geological information. Although Fig. 8 is based on the complete geological data set (Shennan & Horton 2002; Shennan *et al.* 2006) it only shows the sites mentioned in this study.

Clearly visible in these vertical crustal motion maps are the similarities in the primary areas of uplift in Scotland and subsidence in England and Wales. However, the outline of areas undergoing uplift or subsidence in Figs 7(c) and (d) are quite dissimilar in that the map based on solution DDRNF suggests that the whole west coast of Great Britain is rising with respect to the easterly regions of

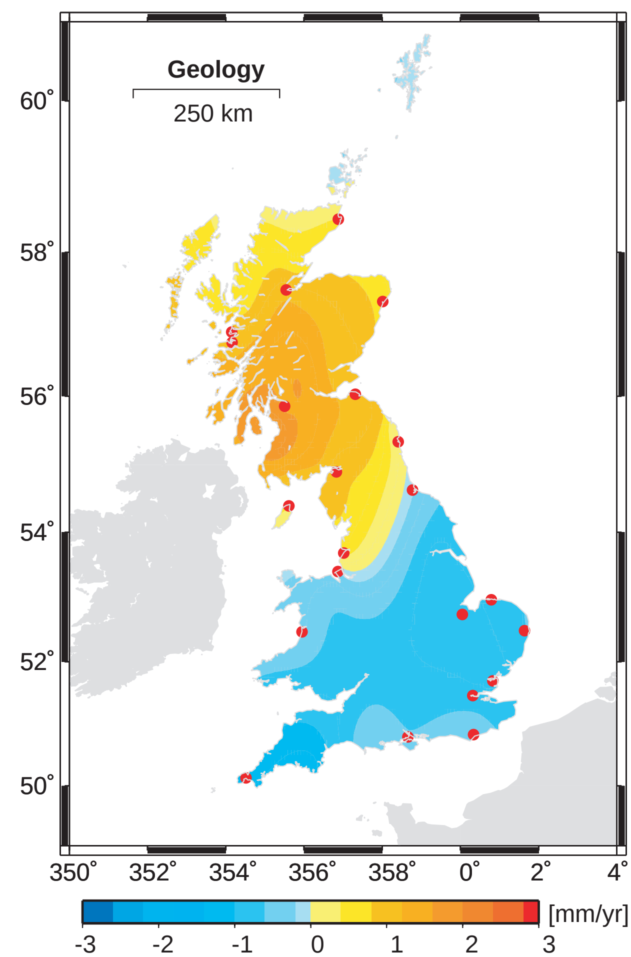

Figure 8. Map of vertical crustal motions derived from Holocene sea level data. Red dots indicate geological sites of Table 4.

England, whereas solution PPPGTF suggests a pattern of uplift and subsidence which is more consistent with that previously published based on Holocene sea level data (Shennan & Horton 2002, Fig. 8).

For solution DDRNF, Figs 7(a) and (c) suggest a possible tilt along a south-westerly to north-easterly axis, i.e. roughly from Newlyn to Lerwick. As this tilt is not apparent in Figs 7(b) and (d), we assume it is due to the regional reference frame implementation which uses IGS stations on the European mainland, all lying in the area to the south and east of Great Britain, and note that this is clearly not being removed through the current AG-alignment procedure.

For solution PPPGTF, Figs 7(b) and (d), the situation is quite different. First, there does not seem to be a network tilt and secondly, it is more difficult to argue in favour of the alignment.

This can be further investigated by directly comparing the AG-aligned CGPS estimates of vertical crustal motions to those from the geological information presented in Table 4. The table gives vertical crustal motions for a number of geological sites, which can be assigned a close-by CGPS station for comparison. We show a comparison of these motions for locations along the western and eastern coasts of Great Britain for solutions DDRNF and PPPGTF in Fig. 9. Figs 9(a) and (b) show the locations from southwest England to western and northern Scotland along the coastlines with the Irish Sea and the Atlantic Ocean and Figs 9(c) and (d) show those from southern England to northeast Scotland along the coastlines with the English Channel and North Sea.

It is worth noting that we should not necessarily expect perfect agreement between the last decade, as represented by the AG-aligned CGPS estimates of vertical crustal motion, and the last 4000 yr (Holocene), as represented by the estimates based on geological studies. Nevertheless, it can be seen that for both CGPS solutions, the AG-aligned CGPS estimates are generally more negative than the geology; with the principal exception of the CGPS@TG station NEWL, which has AG-aligned CGPS estimates of vertical crustal motion which are consistently less negative than those from the geological information and more consistent with those suggested by Gehrels (2006) and Massey *et al.* (2008) (see also Appendix C). Figs 9(b)–(d) do however also suggest a slight overcorrection of the CGPS estimates of vertical station velocity through the current AG-alignment procedure.

Furthermore, we compute the mean offset (and its corresponding standard deviation) and the rms statistic between the CGPS estimates of vertical crustal motion and those from geological

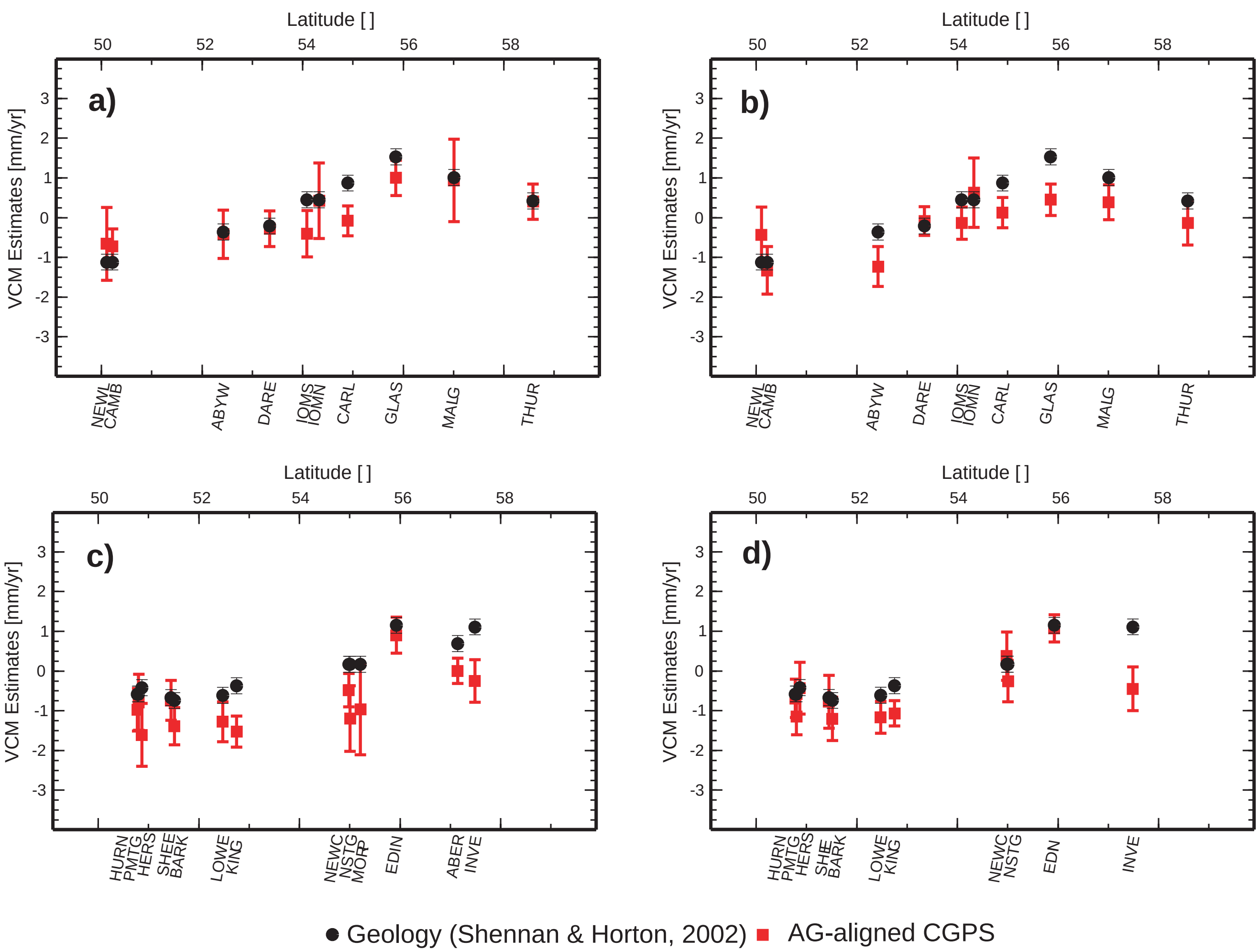

Figure 9. Comparison of AG-aligned CGPS estimates of vertical crustal motions (VCM) from filtered GAS2.4 DD regional network (DDRNF) (a and c) and filtered BSW5.0 globally transformed PPP (PPPGTF) (b and d) coordinate time-series solutions to those from geological information (Shennan & Horton 2002). The top row shows the locations from southwest England along the western coastline to the north of Scotland, whereas the bottom row shows those along the coastlines of the English Channel and the North Sea. Uncertainties are 1σ.

information, and between the AG-aligned CGPS estimates of vertical crustal motion and those from geological information, for solutions DDRNF and PPPGTF. For solution DDRNF we compute mean offsets of $+0.8 \pm 0.5$ and $-0.5 \pm 0.5\,\mathrm{mm\,yr^{-1}}$ and rms of 1.0 and $0.7\,\mathrm{mm\,yr^{-1}}$ for the CGPS and AG-aligned CGPS estimates, respectively. For solution PPPGTF we compute mean offsets of $+0.2 \pm 0.7$ and $-0.4 \pm 0.7\,\mathrm{mm\,yr^{-1}}$ and rms of 0.7 and $0.8\,\mathrm{mm\,yr^{-1}}$ for the two estimates, respectively. This suggests that the AG-alignment procedure does improve the agreement with geological information for solution DDNRF even when the network of stations is expanded from those in Teferle *et al.* (2006) to the current network. This outcome seems at first not to be repeated for the case of solution PPPGTF, where we see an increase in the mean offset and RMS statistic between the geological and the AG-aligned CGPS estimates of vertical crustal motion, when compared to using the CGPS estimates. However, if we take into account the effect of ocean siphoning, as mentioned previously, this would lower all of the geological vertical crustal motion estimates by between 0.2 and $0.4\,\mathrm{mm\,yr^{-1}}$ and hence lead to a further reduction of the mean offsets and rms between the AG-aligned CGPS and geological vertical crustal motion estimates.

We note that this comparison does not account for any differential vertical motions between the sites of the CGPS stations and geological information. If we consider the station separation from Table 4 it is clear that this assumption may not hold true in all cases, and this potentially explains some of the differences seen at GLAS, INVE and IOMS on the western coast and at KING and NEWC on the eastern coast, which suggests that the vertical station velocity estimates at these stations may not represent vertical crustal motions. Interestingly, we can, however, confirm that the vertical station velocity estimates for the CGPS@TG stations do appear to represent vertical crustal motions and that there is no local scale subsidence evident (see Fig. 10).

Fig. 10 also shows that there is no visible correlation between the difference in vertical crustal motion from the AG-aligned CGPS estimates of solution PPPGTF and the geological evidence, with distance between the CGPS station and the geological site, at least up to 50 km.

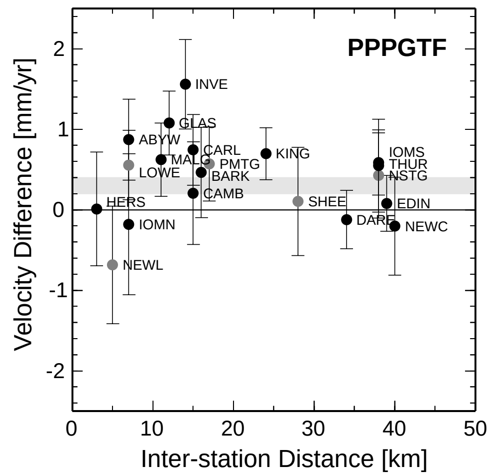

Figure 10. Differences between geodetic and geological vertical crustal motion estimates versus their interstation distances. Differences were computed between the AG-aligned CGPS estimates of vertical crustal motion, from the filtered BSW5.0 globally transformed PPP (PPPGTF) coordinate time-series solution, and those from geological information (Shennan & Horton 2002). Grey circles indicate CGPS@TG stations, and black circles other scientific and network RTK CGPS stations. The grey-shaded area indicates the region of 0.2–0.4 mm $\mathrm{yr^{-1}}$ agreement between the motion estimates if the geological evidence were corrected for ocean siphoning. Uncertainties are 1σ.

5 CONCLUSIONS

Over the last decade the geodetic evidence from CGPS and AG data collected in Great Britain has reached a level of maturity that allows the interpretation of this evidence as present-day crustal motions. Together with estimates of motion using Holocene sea level data from sites close to those of CGPS and AG measurements, we have introduced a comprehensive data set useful for studies of crustal motion information for Great Britain.

We derived horizontal crustal motions for Great Britain from our CGPS estimates of horizontal station velocity under the assumption that the CGPS stations only experience displacements due to horizontal crustal motions. The apparent crustal motion signal follows the predicted motions of the ITRF2000 plate motion model with residual velocities being generally smaller than $1\,\mathrm{mm\,yr^{-1}}$. The residual velocities are apparently random, there is no discernible internal deformation, and they show no dependence on station monumentation or time-series length. Our results do not confirm the previously reported residual motion signal in southeast England.

We derived vertical crustal motions for Great Britain from our CGPS and AG-aligned CGPS estimates of vertical station velocity under the assumption that the CGPS and AG stations only experience displacements due to vertical crustal motions. Overall our results confirmed the expected pattern of subsidence on Shetland, uplift in most areas of Scotland, and subsidence in large areas of England and Wales, and suggest that, in general, the pattern of present-day vertical crustal motions based on geodetic data is consistent with the pattern of vertical crustal motions based on Holocene sea level data, that is, no substantial difference is apparent between the present-day and Holocene vertical motions.

Using the vertical crustal motions from the geological information based on Holocene sea level data we investigated the effectiveness of the AG-alignment procedure to eliminate biases inherent in current CGPS results and the associated estimates of vertical station velocity. With the overall uncertainty associated with current terrestrial reference frames, the AG-alignment clearly provided improved estimates of vertical station velocity for both the regional and global reference frame implementations.

Although we expect further improvements in our CGPS results through a reprocessing of the CGPS data for Great Britain using an updated processing strategy, this will only be possible once the required products have been made available by the IGS. At this stage an inclusion of the new AG station at Herstmonceux will also benefit the computation of the alignment and together with an expansion of the AG station network, a more sophisticated AG-CGPS combination process could be derived.

For now we have provided a comprehensive data set of present-day crustal motions in Great Britain which has already supported the work described in Woodworth *et al.* (2009) and Bradley *et al.* (2009), and highlighted the importance of the complementary nature of the geodetic techniques of CGPS and AG, and of the requirement for independent data sets, that is, the geological information.

ACKNOWLEDGMENTS

The work presented was partly funded through the UK Department for Environment Food and Rural Affairs, the Environment Agency and the Natural Environment Research Council (NERC). The CGPS data from the UK was made available through the NERC funded BIGF (http://www.bigf.ac.uk), all other CGPS data and related GPS products were taken from the IGS (Beutler *et al.* 1999). We also like to acknowledge useful critics and suggestions provided by John Beavan and two anonymous reviewers, which greatly improved the content of this paper.

REFERENCES

Altamimi, Z., Sillard, P. & Boucher, C., 2002. ITRF2000: a new release of the International Terrestrial Reference Frame for Earth science applications, *J. geophys. Res.,* **107**(B10), 2214, doi:10.1029/2001JB000561.

Altamimi, Z., Sillard, P. & Boucher, C., 2004. CATREF software: combination and analysis of terrestrial reference frames, Tech. Rep. LAREG Technical Note SP08, Institut Géographique National, Paris, France.

Altamimi, Z., Collilieux, X., Legrand, J., Garayt, B. & Boucher, C., 2007. ITRF2005: a new release of the International Terrestrial Reference Frame based on time series of station positions and Earth orientation parameters, *J. geophys. Res.,* **112,** B09401, doi:10.1029/2007JB004949.

Aoki, Y. & Scholz, C.H., 2003. Vertical deformation of the Japanese islands *J. geophys. Res.,* **108**(B5), 2257, doi:10.1029/2002JB002129.

Argus, D.F., 2007. Defining the translational velocity of the reference frame of Earth, *Geophys. J. Int.,* **169**(3), 830–838, doi:10.1111/j.1365–246X.2007.03344.x.

Beavan, J., 2005. Noise properties of continuous GPS data from concrete pillar geodetic monuments in New Zealand and comparison with data from U.S. deep drilled braced monuments, *J. geophys. Res.,* **110,** B08410, doi:10.1029/2005JB003642.

Bell, F.G., Donnelly, L.J., Genske, D.D. & Ojeda, J., 2005. Unusual cases of mining subsidence from Great Britain, Germany and Colombia, *Environ. Geol.,* **47**(5), 620–631.

Bennett, R.A. & Hreinsdóttir, S., 2007. Constraints on vertical crustal motion for long baselines in the central Mediterranean region using continuous GPS, *Earth planet. Sci. Lett.,* **257**(3-4), 419–434, doi:10.1016/j.epsl.2007.03.008.

Beutler, G., Rothacher, M., Schaer, S., Springer, T., Kouba, J. & Neilan, R.E., 1999. The International GPS Service (IGS): an interdisciplinary service in support of Earth sciences, *Adv. Space Res.,* **23**(4), 631–635.

Blewitt, G., 2003. Self-consistency in reference frames, geocenter definition, and surface loading of the solid Earth *J. geophys. Res.,* **108**(B2), 2103, doi:10.1029/2002JB002082.

Blewitt, G. & Lavallée, D., 2002. Effect of annual signals on geodetic velocity, *J. geophys. Res.,* **107**(B7), 2145, doi:10.1029/2001JB000570.

Blewitt, G., Davies, P., Gregorius, T.L.H., Kawar, R. & Sanli, U., 1997. Sustainable geodetic monitoring of the natural environment using the IGS, in *Methods for Monitoring Sea Level: GPS and Tide Gauge Benchmark Monitoring and Altimeter Calibration,* pp. 69–83, Jet Propulsion Laboratory, California Institute of Technology, Pasadena.

Blewitt, G. *et al.,* 2006. Geodetic observations and global reference frame contributions to understanding sea level rise and variability, in *Understanding Sea-Level Rise and Variability—A World Climate Research Programme Workshop and a WCRP contribution to the Global Earth Observation System of Systems,* pp. 127–144, World Climate Research Programme, Paris, 6–9 June 2006.

Böhm, J., Niell, A.E., Tregoning, P. & Schuh, H., 2006. Global Mapping Function (GMF): a new empirical mapping function based on numerical weather model data, *Geophys. Res. Lett.,* **33,** L07304, doi:10.1029/2005GL025546.

Bradley, S., Milne, G.A., Teferle, F.N., Bingley, R.M. & Orliac, E.J., 2009. Glacial isostatic adjustment of the British Isles: new constraints from GPS measurements of crustal motion, *Geophys. J. Int.,* in press, doi:10.1111/j.1365-246X.2008.04033.x.

Bruyninx, C., Becker, M. & Stangl, G., 2001. Regional densification of the IGS in Europe using the EUREF Permanent GPS Network (EPN), *Phys. Chem. Earth,* **26**(6–8), 531–538.

Caccamise, D.J., Merrifield, M.A., Bevis, M., Foster, J., Firing, Y.L., Schenewerk, M.S., Taylor, F.W. & Thomas, D.A., 2005. Sea level rise at Honolulu and Hilo, Hawaii: GPS estimates of differential land motion, *Geophys. Res. Lett.,* **32,** L03607, doi:10.1029/2004GL021380.

Calais, E., Han, J.Y., DeMets, C. & Nocquet, J.-M., 2006. Deformation of the North American plate interior from a decade of continuous GPS measurements, *J. geophys. Res.,* **111,** B06402, doi:10.1029/2005JB004253.

Canning, J.C., Henney, P.J., Morrison, M.A., Van Calsteren, P.W.C., Gaskarth, J.W. & Swarbrick, A., 1998. The Great Glen Fault: a major vertical lithospheric boundary, *J. Geol. Soc., Lond.,* **155,** 425–428, doi:10.1144/gsjgs.155.3.0425.

Cardellach, E., Elósegui, P. & Davis, J.L., 2007. Global distortion of GPS networks associated with satellite antenna model errors, *J. geophys. Res.,* **112,** B07405, doi:10.1029/2006JB004675.

Curry, G.B., 1986. Fossils and tectonic along the Highland Boundary Fault in Scotland, *J. Geol. Soc., Lond.,* **143,** 193–198, doi:10.101144/gsjgs.143.1.0193.

Dach, R., Hugentobler, U., Fridez, P. & Meindl, M., eds, 2007. *Bernese GPS Software Version 5.0,* Atronomical Institute, University of Bern, Bern.

de Linage, C., Hinderer, J. & Rogister, Y., 2007. A search for the ratio between gravity variation and vertical displacement due to a surface load, *Geophys. J. Int.,* **171**(3), 986–994.

Dong, D., Yunck, T.P. & Heflin, M.B., 2003. Origin of the International Terrestrial Reference Frame *J. geophys. Res.,* **108**(B4), 2200, doi:10.1029/2002JB002035.

Dong, D., Fang, P., Bock, Y., Webb, F.H., Prawirodirdjo, L., Kedar, S. & Jamason, P., 2006. Spatiotemporal filtering using principal component analysis and Karhunen-Loeve expansion approaches for regional GPS network analysis, *J. geophys. Res.,* **111,** B03405, doi:10.1029/2005JB003806.

Donnelly, L.J., 2006. A review of coal mining induced fault reactivation in Great Britain, *Quart. J. Eng. Geol. Hydrogeol.,* **39,** 5–50.

Edwards, R.J., 2006. Mid- to late-Holocene relative sea-level change in southwest Britain and the influence of sediment compaction, *Holocene,* **16**(4), 575–587.

Ellison, R.A., Woods, M.A., Allen, D.J., Forster, A., Pharoah, T.C. & King, C., 2004. Geology of London. Memoir of the British Geological Survey, Sheets 256 (North London), 257 (Romford), 270 (South London) and 271 (Dartford), England and Wales, British Geological Survey.

Francis, O. *et al.,* 2005. Results of the International comparison of absolute gravimeters in Walferdange (Luxembourg) of November 2003, in *Gravity, Geoid and Space Missions GGSM 2004, IAG International Symposia,* Vol. 129, pp. 272–275, Springer, Heidelberg, Berlin New York, Porto, Portugal. August 30–September 3, 2004.

Fritsche, M., Dietrich, R., Knöfel, A., RüIke, A., Vey, S., Rothacher, M. & Steigenberger, P., 2005. Impact of higher-order ionospheric terms on GPS estimates, *Geophys. Res. Lett.,* **32,** L23311, doi:10.1029/2005GL024342.

Ge, M., Gendt, G., Dick, G., Zhang, F.P. & Reigber, C., 2005. Impact of GPS satellite antenna offsets on scale changes in global network solutions, *Geophys. Res. Lett.,* **32,** L06310, doi:10.1029/2004GL022224.

Gehrels, W.R., 2006. Sea-level rise and coastal subsidence in southwest England, *Reports and Transactions of the Devonshire Association for the Advancement of Science,* **138,** 25–42.

Geirsson, H. *et al.,* 2006. Current plate movements across the Mid-Atlantic Ridge determined from 5 years of continuous GPS measurements in Iceland, *J. geophys. Res.,* **111,** B09407, doi:10.1029/2005JB003717.

Hernández-Pajares, M., Juan, J.M., Sanz, J. & Orús, R., 2007. Second-order ionospheric term in GPS: implementation and impact on geodetic estimates, *J. geophys. Res.,* **112,** B08417, doi:10.1029/2006JB004707.

Hill, T.C.B., Woodland, W.A., Spencer, C.D. & Marriott, S.B., 2007. Holocene sea-level change in the Severn Estuary, southwest England: a diatom-based sea-level transfer function for macrotidal settings, *Holocene,* **17**(5), 639–648.

Hopewell, H., 2003. Environmental and Instrumental Effects of High Precision Gravimetry—a case study in Britain, *PhD thesis,* University of Edinburgh.

Humphries, L., 2001. A review of relative sea level rise caused by mining-induced subsidence in the coastal zone: some implications for increased coastal recession, *Clim. Res.,* **18**(1–2), 147–156.

Johansson, J.M. *et al.*, 2002. Continuous GPS measurements of postglacial adjustment in Fennoscandia 1. geodetic results, *J. geophys. Res.,* **107**(B8), ETG 3/1–3/27.

Kedar, S., Hajj, G.A., Wilson, B.D. & Heflin, M.B., 2003. The effect of the second order GPS ionospheric correction on receiver positions *Geophys. Res. Lett.,* **30**(16), 1829, doi:10.1029/2003/GL017639.

Kierulf, H.P. *et al.*, 2008. Comparison of GPS analysis strategies for high-accuracy vertical land motion, *Phys. Chem. Earth,* **33**(3-4), 194–204, doi:10.1016/j.pce.2006.11.003.

King, R.W. & Bock, Y., 2005. *Documentation for the GAMIT GPS Analysis Software Version 10.2,* Dept. of Earth, Atmospheric, and Planetary Sciences, Mass. Inst. of Technol., Cambridge, USA.

Kreemer, C., Lavallée, D.A., Blewitt, G. & Holt, W.E., 2006. On the stability of a geodetic no-net-rotation frame and its implication for the International Terrestrial Reference Frame, *Geophys. Res. Lett.,* **33,** L17306, doi:10.1029/2006GL027058.

Lambeck, K., 1993a. Glacial rebound of the British Isles I: preliminary model results, *Geophys. J. Int.,* **115,** 941–959.

Lambeck, K., 1993b. Glacial rebound of the British Isles II: a high-resolution, high-precision model, *Geophys. J. Int.,* **115,** 960–990.

Lambeck, K., Johnston, P.J., Smither, C. & Nakada, M., 1996. Glacial rebound of the British Isles III: constraints on mantle viscosity, *Geophys. J. Int.,* **125,** 340–354.

Lambert, A., Courtier, N., Sasagawa, G.S., Klopping, F., Winester, D., James, T.S. & Liard, J.O., 2001. New constraints on Laurentide postglacial rebound from absolute gravity measurements, *Geophys. Res. Lett.,* **28**(10), 2109–2112.

Lambert, A., Courtier, N. & James, T.S., 2006. Long-term monitoring by absolute gravimetry: tides to postglacial rebound, *J. Geodyn.,* **41**(1–3), 307–317.

Langbein, J. & Johnson, H.O., 1997. Correlated errors in geodetic time series: implications for time-dependent deformation, *J. geophys. Res.,* **102**(B1), 591–603, doi:10.1029/96JB02945.

Larson, K.M. & van Dam, T.M., 2000. Measuring postglacial rebound with GPS and absolute gravity, *Geophys. Res. Lett.,* **27**(23), 3925–3928.

Lidberg, M., Johansson, J.M., Scherneck, H.G. & Davis, J.L., 2007. An improved and extended GPS-derived 3D velocity field of the glacial isostatic adjustment (GIA) in Fennoscandia, *J. Geod.,* **81,** 213–230, doi:10.1007/s00190–006–0102–4.

MacMillan, D., 2004. Rate difference between VLBI and GPS reference frame scales, *EOS, Trans. Am. geophys. Un.,* **85**(47), Fall Meet. Suppl., G21B–5.

Mao, A., Harrison, C.G.A. & Dixon, T.H., 1999. Noise in GPS coordinate time series, *J. geophys. Res.,* **104**(B2), 2797–2818.

Massey, A.C., Gehrels, W.R., Charman, D.J., Milne, G.A., Peltier, W.R., Lambeck, K. & Selby, K.A., 2008. Relative sea-level change and post-glacial isostatic adjustment along the coast of south Devon, United Kingdom, *J. Quater. Sci.,* **23**(5), 415–433, doi:10.1002/jqs.1149.

Mazzotti, S., Lambert, A., Courtier, N., Nykolaishen, L. & Dragert, H., 2007. Crustal uplift and sea level rise in northern Cascadia from GPS, absolute gravity, and tide gauge data, *Geophys. Res. Lett.,* **34,** L15306, doi:10.1029/2007GL03020283.

Mazzotti, S., Jones, C. & Thomson, R.E., 2008. Relative and absolute sea level rise in western Candada and northwestern United States from a combined tige gauge-GPS analysis, *J. geophys. Res.,* **113,** C11019, doi:10.1029/2008JC004835.

Milne, G.A., Davies, J.L., Mitrovica, J.X., Scherneck, H.G., Johansson, J.M., Vermeer, M. & Koivula, H., 2001. Space-geodetic constraints on glacial isostatic adjustment in Fennoscandia, *Science,* **291,** 2381–2385.

Milne, G.A. *et al.*, 2006. Modelling the glacial isostatic adjustment of the UK region, *Phil. Trans. Roy. Soc., Part A,* **364,** 931–948, doi:10.1098/rsta.2006.1747.

Mitrovica, J.X. & Milne, G.A., 2002. On the origin of late holocene sea-level highstands within equatorial ocean basins, *Quat. Sci. Rev.,* **21,** 2179–2190.

Mitrovica, J.X. & Peltier, W.R., 1991. On post-glacial Geoid subsidence over the equatorial oceans, *J. geophys. Res.,* **96,** 20 053–20 071.

Mitrovica, J.X., Davis, J.L. & Shapiro, I.I., 1994. A spectral formalism for computing three-dimensional deformations due to surface loads 2. present-day glacial isostatic adjustment, *J. geophys. Res.,* **99,** 7075–7101.

Niebauer, T.M., Sasegawa, G.S., Faller, J.E., Hilt, R. & Klopping, F., 1995. A new generation of absolute gravimeters, *Metrol.,* **32,** 159–180.

Nikolaidis, R.M., 2002. Observation of Geodetic and Seismic Deformation with the Global Positioning System, *PhD thesis*, University of California.

Nocquet, J.M. & Calais, E., 2003. Crustal velocity field of western Europe from permanent GPS array solutions, 1996-2001, *Geophys. J. Int.,* **154,** 72–88.

Nocquet, J.M., Calais, E., Altamimi, Z., Sillard, P. & Boucher, C., 2001. Intraplate deformation in western Europe deduced from an analysis of the International Terrestrial Reference Frame 1997 (ITRF97) velocity field, *J. geophys. Res.,* **106**(B6), 11 239–11 257.

Peltier, W.R., 2001. Global glacial isostatic adjustment and modern instrumental records of relative sea level history, in *Sea Level Rise History and Consequences,*Vol. 75 of International Geophysics Series, p. 232, eds Douglas, B.C., Kearney, M.S. & Leatherman, S.P., Academic Press, San Diego.

Peltier, W.R., Shennan, I., Drummond, R. & Horton, B., 2002. On the post-glacial isostatic adjustment of the British Isles and the shallow viscoelastic structure of the Earth, *Geophys. J. Int.,* **148**(3), 443–475.

Prawirodirdjo, L. & Bock, Y., 2004. Instantaneous global plate motion model from 12 years of continuous GPS observations, *J. geophys. Res.,* **109,** B08405, doi:10.1029/2003JB002944.

Prawirodirdjo, L., Ben-Zion, Y. & Bock, Y., 2006. Observation and modeling of thermoelastic strain in Southern California Integrated GPS Network daily position time series, *J. geophys. Res.,* **111,** B02408, doi:10.1029/2005JB003716.

Shennan, I., 1989. Holocene crustal movements and sea-level changes in Great Britain, *J. Quater. Sci.,* **4,** 77–89.

Shennan, I. & Horton, B., 2002. Holocene land- and sea-level changes in Great Britain, *J. Quater. Sci.,* **17**(5-6), 511–526, doi:10.1002/jqs.710.

Shennan, I., Peltier, W.R., Drummond, R. & Horton, B., 2002. Global to local scale parameters determining relative sea-level changes and the post-glacial isostatic adjustment of Great Britain, *Quatern. Sci. Rev.,* **21**(1-3), 397–408.

Shennan, I., Bradley, S.L., Milne, G.A., Brooks, A., Bassett, S.E. & Hamilton, S., 2006. Relative sea-level changes, glacial isostatic modelling and ice-sheet reconstructions from the British Isles since the Last Glacial Maximum, *J. Quater. Sci.,* **21**(6), 585–599, doi:10.1002/jqs.1049.

Steigenberger, P., Rothacher, M., Dietrich, R., Fritsche, M., Rülke, A. & Vey, S., 2006. Reprocessing of a global GPS network, *J. geophys. Res.,* **111,** B05402, doi:10.1029/2005JB003747.

Stewart, M., Strachan, R.A., Martin, M.W. & Holdsworth, R.E., 2001. Constraints on early sinistral displacements along the Great Glen Fault Zone, Scotland: structural setting, U-Pb geochronology and emplacement of the syn-tectonic Clunes tonalite, *J. Geol. Soc., Lond.,* **158,** 821–830.

Stewart, M.P., Ffoulkes-Jones, G.H., Ochieng, W.Y., Shardlow, P.J., Penna, N.T. & Bingley, R.M., 2002. *GAS: GPS* Analysis Software User Manual. Version 2.4, IESSG, University of Nottingham, Nottingham.

Teferle, F.N., 2003. Strategies for long-term monitoring of tide gauges with GPS, *PhD thesis,* University of Nottingham, Available at: http://etheses.nottingham.ac.uk.

Teferle, F.N., Bingley, R.M., Dodson, A.H. & Baker, T.F., 2002. Application of the dual-CGPS concept to monitoring vertical land movements at tide gauges, *Phys. Chem. Earth,* **27**(32–34), 1401–1406.

Teferle, F.N., Bingley, R.M., Dodson, A.H., Apostoloidis, P. & Staton, G., 2003. RF interference and multipath effects at continuous GPS installations for long-term monitoring of tide gauges in UK harbours, in *Proceedings of the 16th Technical Meeting of the Satellite Division of the Institute of Navigation, ION GPS/GNSS 2003, Portland, Oregon, 9–12 September 2003,* p. 12, Institute of Navigation, Washington, DC.

Teferle, F.N., Bingley, R.M., Williams, S.D.P., Baker, T.F. & Dodson, A.H., 2006. Using continuous GPS and absolute gravity to separate vertical land movements and changes in sea level at tide gauges in the UK, *Phil. Trans. Roy. Soc., Part A,* **364,** 917–930, doi:10.1098/rsta.2006.1746.

Teferle, F.N., Orliac, E.J. & Bingley, R.M., 2007. An assessment of bernese GPS software Precise Point Positioning using IGS final products for global site velocities, *GPS Sols.,* **11**(3), 205–213, doi:10.1007/s10291–006–0051–7.

Teferle, F.N., Williams, S.D.P., Kierulf, H.P., Bingley, R.M. & Plag, H.P., 2008. A continuous GPS coordinate time series analysis strategy for high-accuracy vertical land movements, *Phys. Chem. Earth,* **33**(3–4), 205–216, doi:10.1016/j.pce.2006.11.002.

Tregoning, P. & Van Dam, T., 2005. Atmospheric pressure loading corrections applied to GPS data at the observation level, *Geophys. Res. Lett.,* **32,** L22310, doi:10.1029/2005GL024104.

Van Camp, M., Williams, S.D.P. & Francis, O., 2005. Uncertainty of absolute gravity measurements, *J. geophys. Res.,* **110,** B05406.

van Dam, T.M., Wahr, J., Milly, P.C.D., Shmakin, A.B., Blewitt, G., Lavallée, D. & Larson, K.M., 2001. Crustal displacements due to continental water loading, *Geophys. Res. Lett.,* **28**(4), 651–654.

Vey, S., Dietrich, R., Fritsche, M., Rülke, A., Rothacher, M. & Steigenberger, P., 2006. Influence of mapping function parameters on global GPS network analysis: comparisons between NMF and IMF, *Geophys. Res. Lett.,* **33,** L01814, doi:10.1029/2005GL024361.

Vitushkin, L. *et al.*, 2002. Results of the sixth international comparison of absolute gravimeters, ICAG-2001, *Metrol.,* **39**(5), 407–424.

Wahr, J., Dazhong, H. & Turpin, A., 1995. Predictions of vertical uplift caused by changing Polar ice volumes on a viscoelastic earth, *Geophys. Res. Lett.,* **22**(8), 977–980.

Wdowinski, S., Bock, Y., Zhang, J., Fang, P. & Genrich, J., 1997. Southern California Permanent GPS Geodetic Array: Spatial filtering of daily positions for estimating coseismic and postseismic displacements induced by the 1992 Landers earthquake, *J. geophys. Res.,* **102**(B8), 18 057–18 070, doi:10.1029/97JB01378.

Wdowinski, S. *et al.*, 2004. GPS measurements of current crustal movements along the Dead Sea Fault, *J. geophys. Res.,* **109,** B05403, doi:10.1029/2003JB002640.

Williams, S.D.P., 2003. The effect of coloured noise on the uncertainties of rates estimated from geodetic time series, *J. Geod.* **76**(9–10), 483–494, doi:10.1007/s00190–002–0283–4.

Williams, S.D.P., 2008. CATS: GPS coordinate time series analysis software, *GPS Sols.,* **12**(2), 147–153, doi:10.1007/s010291–10007–10086–10294.

Williams, S.D.P., Baker, T.F. & Jeffries, G., 2001. Absolute gravity measurements at UK tide gauges, *Geophys. Res. Lett.,* **28**(12), 2317–2320, doi:10.1029/2000GL012438.

Williams, S.D.P., Bock, Y., Fang, P., Jamason, P., Nikolaidis, R.M., Prawirodirdjo, L., Miller, M. & Johnson, D., 2004. Error analysis of GPS position time series, *J. geophys. Res.,* **109,** B03412, doi:10.1029/2003JB002741.

Woodworth, P., Teferle, F.N., Bingley, R.M. & Shennan, I., 2009. Trends in UK mean sea level revisited, *Geophys. J. Int.,* **176,** 19–30, doi:10.1111/j.1365–246X.2008.03942.x.

Woodworth, P.L., Tsimplis, M.N., Flather, R.A. & Shennan, I., 1999. A review of the trends observed in British Isles mean sea level data measured by tide gauges, *Geophys. J. Int.,* **136**(3), 651–670.

Wöppelmann, G., Martin Miguez, B., Bouin, M.N. & Altamimi, Z., 2007. Geocentric sea-level trend estimates from GPS analyses at relevant tide gauges world-wide, *Global Planet. Change,* **57**(3-4), 396–407, doi:10.1016/j.gloplacha.2007.02.002.

Wu, X., Argus, D.F., Heflin, M.B., Ivins, E.R. & Webb, F.H., 2002. Site distribution and aliasing effects in the inversion for load coefficients and geocenter motion from GPS data *Geophys. Res. Lett.,* **29**(24), 2210, doi:10.1029/2002GL016324.

Zhang, J., Bock, Y., Johnson, H.O., Fang, P., Williams, S.D.P., Genrich, J., Wdowinski, S. & Behr, J., 1997. Southern California Permanent GPS Geodetic Array: error analysis of daily position estimates and site velocities, *J. geophys. Res.,* **102**(B8), 18 035–18 055.

Zong, Y.Q. & Tooley, M.J., 1996. Holocene sea-level changes and crustal movements in Morecambe Bay, northwest England, *J. Quatern. Sci.,* **11**(1), 43–58.

APPENDIX A: SPATIAL FILTERING

Teferle (2003) found that overall best filtering results were obtained by using as many stations as possible during the bias computation and by carefully selecting and/or excluding individual coordinate components. After close inspection of solutions DDRNU and PPPGTU we selected 20 and 24 stations, respectively, and their coordinate components for the computation of the daily common mode bias (Table 11). Our stations-of-choice were those with long time spans, few coordinate offsets and those not exhibiting any station-specific characteristics, such as unusual or larger periodic signals or features (e.g. the north component of SHEE, Fig. S1). As can be seen, as a result of this selection process, none of the IGS stations located in Great Britain (HERS, HERT, MORP and NPLD) were included to compute the bias. Also, we note that judging from the coordinate time-series for BLAK, COLC and OSHQ, and THUR (Fig. S3), it is unlikely that their additional use in the bias computation for solution PPPGTU had a noticeable effect on the bias compared to solution DDRNU and the filtered coordinate time-series thereafter, as the bias estimate was based on 20 or more stations from early 2000 onwards (Fig. 11). Also, on days with less

Table 11. Station and coordinate components used for the computation of the daily common mode bias.

Station	Component	Station	Component
ABYW	ne-	LEED	neu
BARK	ne-	LERW	neu
BLAK*	neu	LOWE	neu
CAMB	neu	MALG	neu
CARL	neu	NEWC	neu
COLC*	neu	NEWL	neu
DARE	neu	OSHQ*	neu
EDIN	neu	PERS	neu
GLAS	neu	PMTG	neu
IESG	neu	SHEE	−-u
INVE	neu	SUNB	neu
KING	neu	THUR*	neu

Note: Asterisk indicates stations only available to coordinate time-series solution PPPGTU.

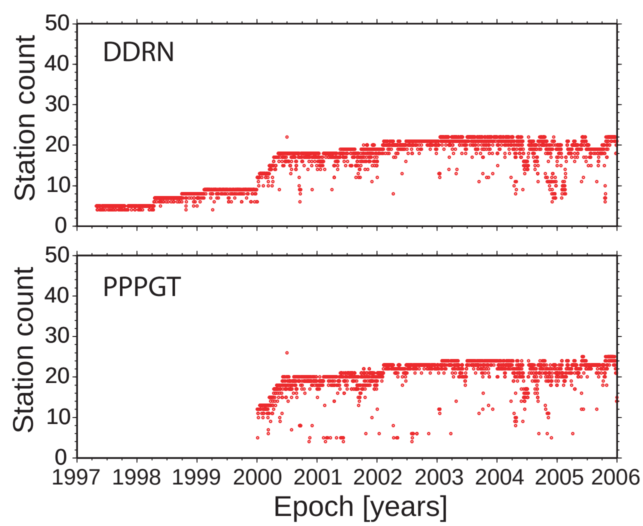

Figure 11. Number of stations used in the computation of the daily common mode bias for the GAS2.4 DD regional network (DDRN) and the BSW5.0 globally transformed PPP (PPPGT) solutions.

than three available stations, we did not compute a common mode bias estimate and for such days, we did not obtain filtered coordinate estimates (Nikolaidis 2002).

APPENDIX B: STABILITY OF CGPS@TG STATION NEWL USED IN THE AG-ALIGNMENT PROCESS

The CGPS@TG station NEWL is founded on the pier at Newlyn tide gauge near to Land's End in southwest England. The stability, in a local and regional context, of NEWL could have an impact on the nature of the apparent systematic offset between the CGPS estimate of vertical station velocity and the AG estimate, which is for the AG station located in the church at Paul about 1.5 km away.

The mean sea level records from the Newlyn tide gauge for the period 1915-21 were used to define Ordnance Datum Newlyn (ODN) and the Tidal Observatory has remained in the same location since that time. The primary tide gauge benchmark (PTGBM) at Newlyn is a bolt, adjacent to the stilling well, inside the Tidal Observatory. The PTGBM was first connected to the primary levelling network in 1915 and was last verified by precise levelling (line G001) in 1990. The TGBM network is effectively formed from seven benchmarks, comprising the PTGBM, two benchmarks on the pier, two benchmarks in the village and two fundamental benchmarks (FBMs), located at Tolcarne, about 900 m northwest of the PTGBM and at Paul, about 1.4 km southwest of the PTGBM. The FBMs are founded on solid rock, whereas all of the other inland benchmarks are Ordnance Survey flush brackets set into walls. The TGBM network was first connected to the PTGBM in 1952 and last verified by precise levelling (line G001) in 1990. The results of the repeated precise levelling surveys showed no significant changes (i.e. less than 0.1 mm) in height within the TGBM network over the period from 1952 to 1990, which suggests that the pier on which the tide gauge and the CGPS@TG station are located did not experience any uplift or subsidence relative to any of the benchmarks, including the two FBMs founded on solid rock, and is stable in a local context.

A further confirmation of this can be obtained for a regional context by considering the vertical station velocities estimated for NEWL along with the vertical station velocities estimated for the scientific CGPS station CAMB, which is at Camborne about 20 km away and founded on solid rock (Table 2). In this respect, it can be reported that the CGPS estimates of vertical station velocity for CAMB were $+0.8 \pm 0.8$ and $+0.5 \pm 0.4$ mm yr^{-1} for solutions DDRNU and DDRNF, respectively, which agree with the estimates for NEWL (Table 7) of $+1.1 \pm 1.1$ and $+0.6 \pm 0.9$ mm yr^{-1} to within 0.3 and 0.1 mm yr^{-1}.

Considering these two different sets of results, therefore, we conclude that the apparent systematic offsets of +1.8, +0.9, +1.4 and +0.9 mm yr^{-1} (Table 9) between the CGPS and AG estimates of vertical station velocity for Newlyn are not due to relative movements between the CGPS@TG station NEWL founded on the pier adjacent to Newlyn tide gauge and the AG station founded on solid rock in the church at Paul, some 1.5 km away.

Unfortunately, a similar assessment cannot be carried out for the AG and CGPS stations at Lerwick on Shetland as similar data to that presented for Newlyn is not available, but at least considering Newlyn, this serves to validate the AG-alignment process carried out.

APPENDIX C: COMPARISONS AT CGPS@TG STATIONS ABER, BRST AND NEWL

For ABER, BRST and NEWL it is possible to compare our vertical station velocity estimates to results from Wöppelmann *et al.* (2007), a recent analysis as part of the IGS TIGA Pilot-Project which used over 200 globally distributed CGPS stations. Their vertical station velocity estimates were computed using the GAMIT (King & Bock 2005) and CATREF (Altamimi *et al.* 2004) software, applying the new absolute satellite and receiver antenna phase centre corrections (Ge *et al.* 2005), new tropospheric delay modelling (Böhm *et al.* 2006) and atmospheric pressure loading corrections (Tregoning & Van Dam 2005). Their reference frame implementation was based on IGb00, so includes an equivalent set of stations as for our implementation in the solutions based on PPPGT. Using a time span of 6.7 years, Wöppelmann *et al.* (2007) computed vertical station velocity estimates for ABER, BRST and NEWL to be 0.2 ± 0.1, -1.2 ± 0.1 and -1.0 ± 0.2 mm yr^{-1}, respectively. When comparing these to our CGPS and AG-aligned CGPS estimates (Tables 7 and 10), we show a reduction in the velocity differences for ABER, BRST and NEWL from +1.1, +2.5, and +1.7 mm yr^{-1} to −0.2, +1.2 and +0.4 mm yr^{-1}, respectively for solution DDRNF, and for NEWL from 1.2 to 0.6 mm yr^{-1} for solution PPPGTF. Again, this serves to validate the AG-alignment process carried out.

SUPPORTING INFORMATION

Additional Supporting Information may be found in the online version of this article:

Appendix S1. Three supplementary tables and four supplementary figures, which are referred to in the text.

Please note: Wiley-Blackwell are not responsible for the content or functionality of any supporting materials supplied by the authors. Any queries (other than missing material) should be directed to the corresponding author for the article.